

CONTRIBUTION OF ARTIFICIAL PROPRIOCEPTION ON COORDINATED
MANIPULATION

by

Mehdi Hojatmadani

B.S., Mechanical Engineering, Central Tehran Azad University, 2013

Submitted to the Institute for Graduate Studies in
Science and Engineering in partial fulfillment of
the requirements for the degree of
Master of Science

Graduate Program in Mechanical Engineering
Boğaziçi University

2016

CONTRIBUTION OF ARTIFICIAL PROPRIOCEPTION ON COORDINATED
MANIPULATION

APPROVED BY:

Assist. Prof. Dr. Evren Samur
(Thesis Supervisor)

Assoc. Prof. Dr. Burak Güçlü

Assist. Prof. Dr. Ayşe Küçükylmaz

DATE OF APPROVAL: 15.07.2016

ACKNOWLEDGEMENTS

I would like to thank my supervisor Prof. Evren Samur who helped me through the way with his ideas and motivated me to be the academic person I am. Secondly I would like to thank Prof. Ayşe Küçükylmaz and Prof. Burak Güçlü who accepted to be jury members of my master's thesis.

My appreciation also goes to my friends in haptics and robotics lab including Gholamreza, Mohamad, Efe, Alican and Taylan and my good friends out of the lab Mehdi Emadian, Pouya Yousefi, Alireza Ahmadi, Aydin Sheykhi, Abdulkadir, Serkan and every single person who helped me during my studies.

Last but not least my special love and gratitude to my family who have borne a lot so I can achieve what I've gained so far, to my lovely mom Soudabeh to my kind dad Saied and to my sister Maryam, who is also my good friend.

ABSTRACT

CONTRIBUTION OF ARTIFICIAL PROPRIOCEPTION ON COORDINATED MANIPULATION

Lacking an efficient sensory feedback system has caused upper-limb robotic prostheses to lose their popularity among users as they cannot reflect realistic feeling of performing a task. One of the obstacles in achieving this realism is missing proprioceptive feedback, which is the sense of relative position, velocity and kinesthetic force of neighboring parts of the body. It has been proved that proprioception plays an important role in body coordination during movements. Identifying the exact contribution of artificial proprioception on coordinated manipulation is a keynote in the research field yet to be explored. In order to study artificial proprioception, we have developed a novel virtual-reality-based experimental setup comprising of a two degrees of freedom (DOF) haptic device and an input device working with a virtual environment. Later, we conducted a psychophysical test in which subjects compared real and virtual springs with different stiffness constants. Results showed that the setup was able to render intended stiffness with high success rate. Eventually, a psychophysical test was conducted. An unstable task called “Strength-Dexterity Test”, based on buckling of compression springs, has been employed. Relative contributions of vision, position and force and their sensory substitution method on feedback control was quantified with this 2-DOF task. Subjects interacted with a virtual spring with the index finger of their dominant hand through either the haptic interface, the input device, or a force sensor. Therefore, input condition were either isotonic (when the haptic device or the input device is used and the finger moves) or isometric (when the force sensor is used and the finger is stationary). Three feedback conditions were tested: visual only, wrong- modality sensory substitution of position and force (through vibration) and modality-matched sensory substitution. Results show that modality matched sensory substitution feedback did not have a notable effect on subjects’ performance.

ÖZET

YAPAY PROPRIOSEPSİYONUN KOORDINE HAREKET ÜZERİNDEKİ KATKISI

Etkili duysal geribesleme sistemi eksikliği üst ekstremitelerde robotik protezlerinde kullanıcılar üzerindeki popülaritesinin azaltılmasına neden oluyor çünkü bunlar bir görevi yerine getirmenin gerçekçi hissini yansıtamıyor. Bu realizmi başarmaktaki engellerden bir tanesi propriyosepsiyon geribeslemesinin eksikliğidir, (göreceli pozisyon, hız ve vücuttaki komşu parçaların kinestetik kuvveti algısı). Propriyosepsiyonun vücut koordinasyonunda birden fazla eklem hareketinin olduğu yerlerde önemli bir rol oynadığı ispatlanmıştır. Yapay propriyosepsiyonu çalışmak için iki serbestlik dereceli haptik cihazından ve sanal ortamda çalışan girdi cihazından oluşan deneysel düzenek odaklı yeni bir sanal gerçeklik geliştirdik. Daha sonra, deneklerin gerçek ve sanal yayları farklı sertlik sabitleriyle kıyasladığı bir psikofizik test yaptık. Sonuçlar gösteriyor ki deney düzeneği planlanan sertlik değerini yüksek başarı oranıyla simüle edebiliyor. Çalışmanın son aşamasında psikofizik test yapıldı. Strength-Dexterity olarak adlandırılan kararsız/dengesiz görev, basma yayının bükülmesinden/burkulmasından baz alınarak uygulandı. Görme, propriyosepsiyon ve yapay propriyosepsiyonun geribeslemeli kontrol üzerindeki göreceli katkıların iki serbestlik dereceli görevle niceliği belirtilmiştir. Denekler sanal bir yayla baskın ellerinin işaret parmaklarıyla haptik arayüzü, girdi cihazı ya da kuvvet sensörü aracılığıyla etkileşim içerisine girmiştir. Bu yüzden girdi koşulu ya izotonik (haptik cihazı ya da girdi cihazı kullanıldığında ve parmak hareket ettiğinde) ya da izometrik (kuvvet sensörü kullanıldığında ve parmak hareketsizken). Üç geribesleme durumu test edilmiştir, sadece görsel, yanlış propriyosepsiyonun sensory substitution ve doğru yapay propriyosepsiyon. Sonuçlar gösteriyor ki yapay propriyosepsiyon geribeslemesi deneklerin performansı üzerine dikkate değer bir tesir bırakmamıştır.

TABLE OF CONTENTS

ACKNOWLEDGEMENTS	iii
ABSTRACT	iv
ÖZET	vi
LIST OF FIGURES	ix
LIST OF TABLES	xv
LIST OF SYMBOLS	xvi
LIST OF ACRONYMS/ABBREVIATIONS	xvii
1. INTRODUCTION	1
1.1. Motivation	1
1.2. Aims	3
1.3. Outline	4
2. LITERATURE REVIEW	5
2.1. Types of Upper-limb Protheses	6
2.2. Proprioception	11
2.3. Sensory Substitution	17
2.4. Virtual Reality for Protheses and Rehabilitation	25
3. METHODOLOGY	29
3.1. Experimental Setup	30
3.1.1. Hardware	30
3.1.2. Virtual Environment	34
3.1.3. Buckling Model	40
3.2. Experimental Protocol	42
4. HAPTIC INTERFACE	49
4.1. Electro-mechanical Design	49
4.2. Control Algorithms	50
4.2.1. Admittance Control	52
4.2.2. Impedance Control	53
4.3. Evaluation	54
4.3.1. Physical Evaluation	54

4.3.1.1.	Friction Compensation	54
4.3.1.2.	Static Response	55
4.3.1.3.	Input-Output Curve	56
4.3.2.	Psychophysical Evaluation	57
4.3.2.1.	Subjects	58
4.3.2.2.	Procedure	58
4.3.2.3.	Results	59
5.	RESULTS AND DISCUSSIONS	61
5.1.	Results of Psychophysical Study	61
5.2.	Discussion	63
6.	CONCLUSION	68
6.1.	Contributions	68
6.2.	Future Works	69
	REFERENCES	70

LIST OF FIGURES

Figure 1.1.	Compressing a spring with endcaps in key pinch. Three possible configuration of compression spring. Compressing a compression spring requires coordination of both force magnitude and the alignment of applied forces. In case of successful compression, spring will reach to its solid length (middle picture) other wise it buckles (right picture) [12].	3
Figure 2.1.	Levels of upper limb amputation [19].	6
Figure 2.2.	Different kinds of available prostheses. In a body-powered prosthesis, the device performs grasping action based on gross movement of shoulder which is transmitted to the gripper through a cable (Bowden cable). The cable in turn transmits reaction forces from the hand/hook to the body, hence providing a sensory awareness of the prosthesis. In a myoelectric prosthesis, the signals recorded from muscles are processed to perform user's desired movement. Their main disadvantage is lack of sensory feedback except for those such as motor sound or accidental stimulations. A cosmetic passive hand is used to simply just compensate for appearance deficiency of a lost limb but does not utilize any electronic feature [17].	8
Figure 2.3.	Commercially available myoelectric prostheses [19].	9
Figure 2.4.	Control process of a myoelectric prosthesis with sensory feedback [40].	11
Figure 2.5.	Mechanoreceptors in the skin [55].	13

- Figure 2.6. A schematic of various modalities of proprioception. Somatosensory senses are considered the conscious constituent of proprioception whereas neuromuscular control is carried out in unconscious level [60]. 14
- Figure 2.7. Hand path and reversal trajectory errors in healthy people (left) and deafferented patients (right) [8]. 15
- Figure 2.8. Powerball. The Powerball is a gyroscope that will apply a multi-directional inertia on the wrist muscles when activated. Its goal is to stimulate an unconscious proprioception rehabilitation through a reactive muscle activation.[60] 16
- Figure 2.9. An example of artificial proprioception feedback in a grasping task. (a) Subject moves the virtual hand via force sensor and receives motion feedback via the designed haptic device (behind cloth) and a desktop computer. (b) Haptic device measures a grasping force input via the force sensor at the thumb to determine the movement of the virtual hand. [15] 17
- Figure 2.10. General layout for providing sensory feedback. In sensing transduction stage physical stimuli is converted from one form of energy to another which is more proper. Later a decoding algorithm identifies important sensory state components which will be used by an encoding algorithm to transform them into easily interpreting output signals. Eventually in the output stage obtained signal is converted to a form of energy to be applied on body sensory system.[17] . . . 18

Figure 2.11.	Vibrotactile feedback device. Here vibration feedback is delivered to subject in three ways; tactor can be placed under the finger(a), it can also be bandaged to subject’s upper arm(b) alternatively it can be attached to ball of the foot [91].	20
Figure 2.12.	An example of a mechanotactile feedback haptic display. A. Experimental setup during mechanotactile experiments. B. Vibrotactile stimulator C. Mechanotactile stimulator; motor rotation is converted to a normal force on the skin [95].	22
Figure 2.13.	Mechanotactile feedback utilizing skin stretch method. fingertip skin deformation devices employed in sensory subtraction [99]. . .	23
Figure 2.14.	Auditory sensory feedback. Experimental setup in which the subject controls the robotic hand in grasping a soda can using myoelectric signals and auditory feedback to successfully adjust grasping force [78].	24
Figure 2.15.	Concept, Algorithm and setup of an audio-visual sensory substitution system. A) Musical instrument used to represent color e.g. white is mapped to a choir and black to silence B) Visuo-auditory sensory substitution instances C) The EyeMusic application used on a laptop D) Sample setup equipped with camera on a sunglasses and earphones [107].	24
Figure 2.16.	Examples of virtual reality systems in haptics [113].	26
Figure 2.17.	pretesting assembly environment mode of SPARTA in a puzzle assembly task.[116]	27

Figure 2.18.	Experimental setup. Two cutaneous devices had to be worn by subjects on each hand, they let users control pliers via multiple Omega7 devices. (a) General overview of setup. (b) Detail of one hand wearing the devices. (c) Virtual environment with surgical pliers [99].	28
Figure 2.19.	Simulation implementation in SOFA. (a) Virtual training in cardiac electrophysiology, (b) patient-specific planning of cryosurgery (c) intra-operative guidance for laparoscopy [122].	28
Figure 3.1.	Input device (left) and haptic interface (right).	31
Figure 3.2.	General design of haptic device (right), and input device (left). . .	32
Figure 3.3.	Force sensor ATI Nano-17 used as an isometric input device. . . .	33
Figure 3.4.	Combination of multiple sinusoidal waves in time domain. (a) Beat combination of two waves with equal amplitude A and different frequencies ω_1 and ω_2 results in a sinusoid with angular speed ω_M which is equal to the average between ω_1 and ω_2 , and an amplitude of $2A$ which is modulated by a sine having angular speed ω_{LF} half the difference between ω_1 and ω_2 . (b) Sum of three vibrations, two of which similar and the third with equal amplitude but different angular speed. This time the envelope modulates at twice ω_{LF} . (c) Sum of three vibrations with equal amplitude but different frequencies: all combinations of frequencies contribute to the output waveform [83].	34
Figure 3.5.	Time domain measurement and frequency content of a vibration actuation with duty cycle of 63% and 74%.	35

Figure 3.6.	Hierarchical representation of our developed virtual reality model.	37
Figure 3.7.	A virtual spring controlled by the haptic interface in translation (along Y axis) and rotation (around Z axis) degrees of freedom. . .	41
Figure 3.8.	Graphical representation of buckling stability. As the angle is more deviated from zero value, allowable applying force is more limited hence increase probability of spring buckle [5].	43
Figure 3.9.	Psychophysical test. Subject is interacting with input device and is receiving force feedback on his contralateral hand index finger. Subject reached the goal position.	46
Figure 3.10.	Psychophysical test. Subject is interacting with force sensor to compress the virtual spring.	47
Figure 4.1.	Designed mechanism of haptic device. Rotational movement of the motors are transformed to a combination of translation and rotation of the plate.	50
Figure 4.2.	Technical design of haptic device including all the components. . .	51
Figure 4.3.	Spring cap free body diagram.	51
Figure 4.4.	Admittance control block diagram.	53
Figure 4.5.	Impedance control block diagram.	54
Figure 4.6.	Resistive forces without compensation (Orange) and with friction compensation (Blue).	55

Figure 4.7.	Device input versus force output with friction compensation. . . .	57
Figure 4.8.	Virtual spring simulation. Solid line and shaded area represent the mean and the standard deviation of the five measurements, respectively. Arrow indicates the direction of movement	58
Figure 4.9.	The input device (left) has isotonic input capability and the haptic interface (right) is an impedance-type device	60
Figure 5.1.	Mean values of number of trials before achieving the learning condition	61
Figure 5.2.	Success rates for each mode of the experiments.	63
Figure 5.3.	Participants' success rate based on input mode and sensory substitution method.	64
Figure 5.4.	Mean value of error distance. Horizontal axes are the modes of experiment, vertical axes are the corresponding error distance values.	65
Figure 5.5.	Elapsed Time for Successful Trials in Main Session.	67
Figure 5.6.	Mean value of subjects' difficulty rating	67

LIST OF TABLES

Table 2.1.	Characteristics of commercially available prosthetic hands [19].	9
Table 3.1.	SOFA components	38
Table 3.2.	Different modes of psychophysical experiment. Modes; (1) Isotonic input with force feedback, (2) Isotonic input without force feedback, (3) Isometric input without position feedback, (4) Isotonic input with vibration feedback, (5) Isometric input with vibration feedback, (6) Isotonic input with sensory substitution of force, and (7) Isotonic input with sensory substitution of position.	47
Table 3.3.	Experimental procedure for different modes of the psychophysical test	48
Table 4.1.	Intended and measured spring stiffness	57
Table 4.2.	Experimental Setup Results	59
Table 5.1.	ANOVA results and Post Hoc analysis for number of trials in training	62
Table 5.2.	ANOVA results and Post Hoc analysis for success rate in main session	62
Table 5.3.	Results of two-way ANOVA.	63
Table 5.4.	ANOVA results and Post Hoc analysis for distance error	66
Table 5.5.	ANOVA results.	66

LIST OF SYMBOLS

a_m	Acceleration of master robot
a_s	Acceleration of slave robot
E	Modulus of Elasticity
\mathcal{F}	Function Symbol
f_i	Different force functions
G	Modulus of Rigidity
J	Jacobian
K_d	Derivative Controller Coefficient
K_p	Proportional Controller Coefficient
M	Moment
v_m	Velocity of master robot
v_s	Velocity of slave robot
x_m	Position of master robot
x_s	Position of slave robot
ν	Poisson's Ratio
ϕ	Phase Shift
ω	Angular Velocity
ω_1	First Frequency
ω_2	Second Frequency
ω_{LF}	Lower Frequency Tone
ω_M	Mean Frequency
Θ	Spring Endcap Angle
$\dot{\Theta}$	Spring Endcap Angular Speed

LIST OF ACRONYMS/ABBREVIATIONS

2D	Two Dimentional
A	Amp
AC	Alternative Current
ASCII	American Standard Code For Information Interchange
BP	Body Powered
CBM	Constraint Based Modeling
CHAI3D	Computer Haptics and Active Interfaces
COM	Communication
DC	Direct Current
DOF	Degree of Freedom
FMG	Force Myography
fMRI	Functional Magnetic Resonance Imaging
FTDI	Future Technology Devices International
GPU	Graphic Processing Unit
GUI	Graphical User Interface
HSD	Honest Significant Difference
IBM	International Business Machine
ICMS	Intracortical Microstimulation
ICSP	In-Circuit Serial Programming
IMES	Implantable Myoelectric Sensors
LCD	Liquid Crystal Display
LED	Light Emitting Diode
mA	Milliamp
MCP	MetaCarpophalangeal Joint
MHz	Mega Hertz
mm	Millimeter
NI	National Instrument
ODE	Open Dynamics Engine

PBM	Physically Based Modeling
PC	Personal Computer
PCI	Peripheral Component Interface
PD	Proportional Derivative
PLIC	Posterior Limb of the Internal Capsule
PPC	Posterior Parietal Cortices
PWM	Pulse Width Modulation
RMA	Reactive Muscle Activation
sEMG	Surface Electromyography
SOFA	Simulation Open Framework Architecture
SPARTA	Scriptable Platform for Advanced Research in Training and Assembly
SPIDAR	Space Interface Device for Artificial Reality
SPSS	Statistical Package for the Social Sciences
TVSS	Tactile Vision Sensory Substitution
TMR	Targetted Muscle Reinnervation
USB	Universal Serial Bus
UART	Universal Asynchronous Receiver/Transmitter
V	Volt
VPS	Voxmap PointShell
WHO	World Health Organization

1. INTRODUCTION

1.1. Motivation

In 2009, hospital costs associated with amputation totaled more than \$8.3 billion. It is projected that the number of people living with the loss of a limb will be more than double by the year 2050 to 3.6 million [1]. Increasing number of amputees in the upcoming years necessitates substitution for the lost limb to increase their quality of life. Although there are solutions like transplantation and replantation, prosthetic devices seem to be the most promising solution as there are noninvasive and can be removed or mounted upon user's desire. Different kinds of prostheses have been developed for upper-limb amputation but lacking an efficient sensory feedback system has caused these prostheses to lose their popularity among users as they cannot reflect realistic feeling of performing a task. Here lies the most critical setback of commercially available prostheses. Dudkiewicz et al. [2] reported that rejection rate in body-powered and electric-powered prostheses % 29 and % 30 respectively. The main reasons described for prosthesis rejection were dissatisfaction with prosthetic comfort, function and control [3]. In spite of the advances in prostheses development, the main problem which is lack of realistic sensory information still exists.

Humans do not have dedicated mechanoreceptors to identify the properties of the dynamic systems, such as stiffness or damping, so they must combine information from force mechanoreceptors and proprioceptors to relate changes in applied forces to changes in position [4]. Hence, deficits in proprioceptive feedback can disable one from performing a wide variety of movements and tasks. Insufficient effort in studying the role of proprioception and its contribution in successful manipulation has led to current challenges in prosthetic hand control. Another issue to be discussed is simplifying hypotheses in available studies which consider position information of body as proprioception while proprioception includes both position and force information. Another rationale to conduct a study in this field was that almost all available studies on proprioception were limited to single-DOF tasks while a wide variety of daily tasks

and movements require multijoint movements which are performed in multiple-DOF.

Consequently, we devised a virtual task which not only relies on appreciation and control of limbs but also highly depends on coordination of applied forces in 2-DOF. Our study benefits from a task called “Strength-Dexterity” [5] which evaluates subjects’ ability in controlling their fingers position as well as their exerted force. “Strength-Dexterity” relies on principle of buckling of compression spring (an example is shown in Figure 1.1). Buckling of compression spring can be mathematically modeled based on bifurcation theory. Bifurcation studies changes in the qualitative or topological structure of a given class such as integral curves and the solutions of a group of differential equations. An eminent application of this theory is in study of dynamic systems, a bifurcation occurs when a minimal change in the parameters (the bifurcation parameters) of a system leads to a sudden ‘qualitative’ or topological change in system behavior.

Proprioception provides central nervous system with information about the spatial location of body parts. It has been proved that proprioception plays an important role in body coordination during movements where more than one joint moves [2, 6]. A wide variety of experiments has been conducted with able-bodied subjects, investigating human hand and finger capabilities. A series of experiments were conducted by Cuevas et al. [7–11] on force exertion and positioning capabilities of human hand. A challenging task demonstrating human sensorimotor ability to adjust finger motion and force is dynamic precision pinch [9]. We implemented a virtual task based on “Strength-Dexterity Test” [9–11]. In another work, Gurari et al. [12] developed a 1-DOF haptic interface in which they intended to compare the contribution of visual and proprioceptive motion feedback on a successful manipulation of a virtual hand. Subjects tried to perform a targeted motion task. Blank et al. [13] revised the former experiment in which different sensory information was delivered in different trials compared to their first design where proprioception and force feedback were delivered simultaneously. Their results indicated that targeting performance was elevated with proprioceptive feedback under non-sighted condition and some sighted conditions as well. In literature, studies with computer input devices for virtual environments, decoupled positioning and force control tasks and focused on single-DOF manipulations [5, 13–

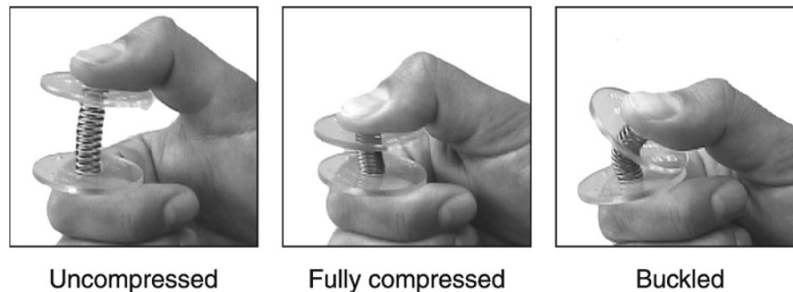


Figure 1.1 Compressing a spring with endcaps in key pinch. Three possible configuration of compression spring. Compressing a compression spring requires coordination of both force magnitude and the alignment of applied forces. In case of successful compression, spring will reach to its solid length (middle picture) otherwise it buckles (right picture) [12].

15]. For example, Zhai and Milgram showed that users' performance on virtual object positioning is worst with isometric devices than isotonic ones when position control is employed [16]. One of the reasons for this degradation is the lack of position feedback in isometric condition. No study has been conducted on a dynamic task in which both position and force information are available to subjects.

In this study, we investigate how able-bodied subjects perform at a multi-DOF manipulation task with isotonic and isometric control when position and force feedback is substituted for the missing sensory information. Since this task highly depends on coordination of force and position at the same time, its virtual implementation provides a novel platform to test contributions of sensory feedback on coordinated manipulations.

1.2. Aims

Aim 1. To develop a 2-DOF haptic interface which will be utilized in a series of psychophysical experiments to determine contributions of vision, sensory substitution feedback of force and position on task completion of manipulation of a virtual object. We developed a haptic interface interacting with a virtual environment. This configu-

ration lets us study different manipulation tasks in two operational modes of muscle, isometric and isotonic modes, and provided position or force feedback. This interface was used later to carry out our designed tasks on subjects.

Aim 2. To test whether sensory substitution of position and force contributed to successful manipulation of unstable objects in multi-DOF. To achieve this goal we utilized the interface developed in the first step. We carried out the experiment with able-bodied people. Unstable object manipulation needs to be performed with feedback therefore by implementing appropriate strategies we were able to measure the contribution of vision, sensory substitution feedback of position and force on task completion. Experiments were performed by index finger of the subjects which was placed on the haptic interface. Feedback was delivered to contralateral index finger through the another device which had been developed. We designed tasks which included both modes of finger muscle operations.

1.3. Outline

In the following sections design; a thorough review of the research conducted regarding this topic is carried out. On subsequent sections, development and evaluation of our experimental setup are explained, the psychophysical experiments are discussed and the results are presented. Eventually discussion and conclusion are conducted and rationale of the results is presented.

2. LITERATURE REVIEW

Human have always relied on their senses to acquire an understanding of their environment and other people's feelings. Our senses are the only informatory channels which help us build our conception of the world we live in. Losing any of these sensory inputs will cause catastrophic results in a person's life. Amputation is one of those impairments which not only forces a physical difficulty to the amputee's life but also hinders person's sensory understanding of his surrounding. Here lies one of the main branches of robotics and haptics in which researchers try to recreate lost sensory experience.

Although modern haptics, as a classified field of study, is comparatively a newly born branch of science it has progressed rapidly due to advances in electrical, mechanical and computer engineering. One of the emerged topics which has drawn researchers' attention, is upper-limb robotic prostheses and inclusion of sensory feedback in the state-of-the-art upper-limb prostheses. Despite the great amount of effort and research [17] such goal has not been achieved yet as this topic requires a great deal of interdisciplinary understanding of human hand functioning and available technology to be utilized in simulating such complicated biological systems.

Being able to interact with surrounding as easily as a healthy person is a demand of upper-limb amputees and individuals with congenital upper-limb deficiencies [18]. Our sensory system sends information about four major modalities to the central nervous system including touch, proprioception, pain and temperature [17]. Amputees are deprived from these senses up to certain extent based on their level of amputation. Upper-limb amputation can be categorized based on the level of limb absence as transcarpal, wrist disarticulation, transradial, elbow disarticulation, transhumeral, shoulder disarticulation and forequarter as illustrated in Figure 2.1 [19]. Prostheses are often described to be a foreign tool by the users as they can not deliver somatosensory feedback. Except being used for manipulating objects prostheses do not give a sense of ownership to their users especially in the absence of eye contact with the prosthesis

[20].

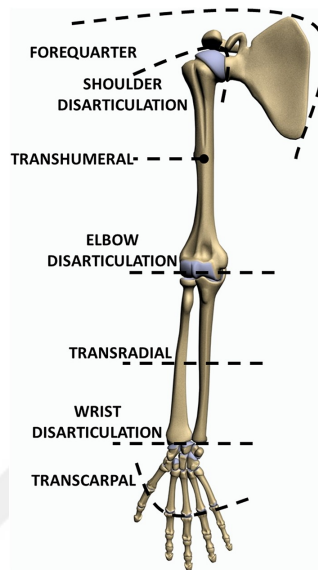


Figure 2.1 Levels of upper limb amputation [19].

Currently available prostheses are short of having a sufficient configuration and motion feedback and this necessitates constant eye contact with the prosthesis which is not convenient and sometimes not even possible [15].

In order to achieve the aims mentioned in Section 1.2, the related studies have been reviewed. The following chapter covers the highlights of these studies which were beneficial in different steps of our way.

2.1. Types of Upper-limb Prostheses

Three types of prostheses are presently available for upper limb amputees. First, body-powered and cable operated mechanisms with a split hook or hand as a terminal device; second, electrically powered prostheses controlled by muscle sensors (myoelectric) or by micro switches; and third, cosmetic replacements with passive hands appeared in Figure 2.2 [21]. Body-powered prostheses, are controlled by gross movements of user's own body. A Bowden cable is used to transmit forces produced by body movements to a terminal device: either a split hook or a mechanical hand [17].

In technologically advanced battery-powered prostheses, a wide variety of methods are implemented to create an intuitive functionality. Among non-invasive empirical methods we can name; analyzing signals extracted from surface electromyography (sEMG) [22], ultrasound imaging [23] and force myography (FMG) [24]. There are invasive methods presented in the literature as well. These include Implantable Myoelectric Sensors (IMES) [25], neural interfaces [26] from peripheral or central nervous system as well as targeted muscle reinnervation (TMR). Patients who underwent TMR surgery were able to feel an expression of the hand map as if they were touched on the missing limb [27]. One of the drawbacks of this method however, is its exclusiveness as there is a limited number of institutions performing TMR surgeries. In 2013, just 40 patients underwent TMR operation [28]. Another issue with TMR method is the difficulty in replicating proprioceptive sensation through connections to peripheral nervous system due to the nature of proprioception which is multifaceted, spatially distributed and complex [29].

Generally there are five factors pivotal in design of any kind of prosthesis whether body-powered or myoelectric including: control, function, feedback, cosmesis and user satisfaction [30]. A conventional upper-limb robotic prosthesis usually faces sensory shortcomings like; a complete lack of proprioception due to absence of position and velocity of limb segments and a partial lack of exteroception due to unavailability of any haptic feeling of temperature, force, shape and texture [31].

Most available devices, demand training and sensory adaptation to decode an external stimulus as exteroceptive or proprioceptive information (e.g. conceiving vibration as force)[32]. A critical property of an effective stimulus is that it must first input the appropriate stimulus, and secondly make sure that the feedback signal is delivered as a natural feedback and not as a distraction. It has been shown that adding a BioTac sensor to a normal robotic hand and a haptic display to replay measured stimuli can lead to the development of an Upper-limb prosthetic hand which helps users be more aware of the environment [33]. Awkward and aberrant movements which are not

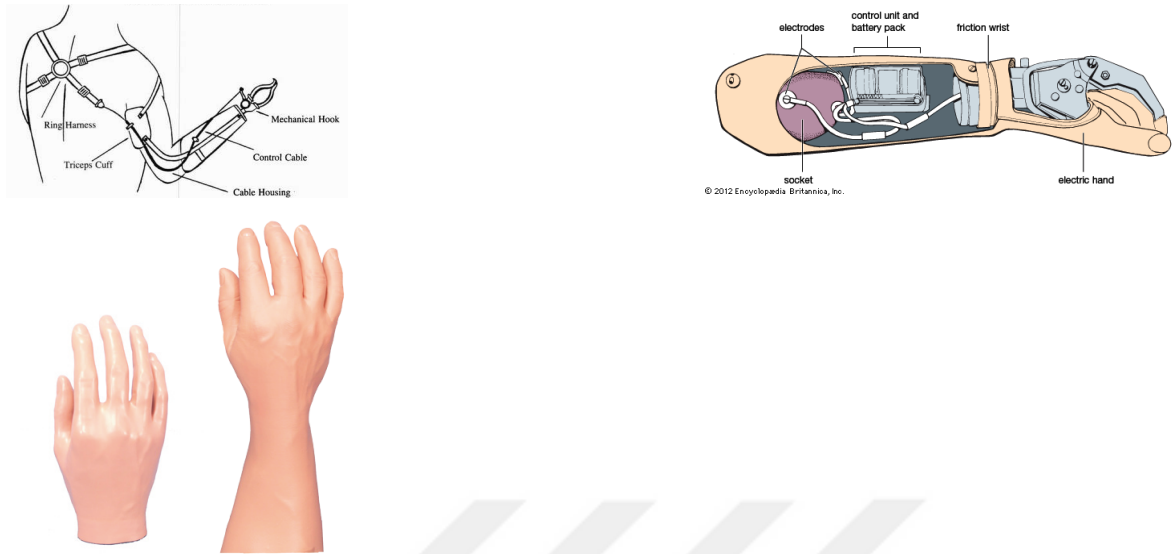


Figure 2.2 Different kinds of available prostheses. In a body-powered prosthesis, the device performs grasping action based on gross movement of shoulder which is transmitted to the gripper through a cable (Bowden cable). The cable in turn transmits reaction forces from the hand/hook to the body, hence providing a sensory awareness of the prosthesis. In a myoelectric prosthesis, the signals recorded from muscles are processed to perform user's desired movement. Their main disadvantage is lack of sensory feedback except for those such as motor sound or accidental stimulations. A cosmetic passive hand is used to simply just compensate for appearance deficiency of a lost limb but does not utilize any electronic feature [17].

felt by healthy persons can be experienced by prostheses users due to limited function of prostheses [34]. These aberrant movements have been stated as one of the reasons of prosthesis rejection [35]. Users' priorities for a better prosthetic hand for both body-powered and myoelectric prostheses are; wrist movement, improved movement mechanisms which need less visual attention and being able to coordinate motions of two joints [18].

The current devices lack an intuitive control strategy which requires less visual attention and allows for coordinated movements of two joints[30]. There are intrinsic differences both in structure and in mechanism of body-powered and myoelectric prostheses. This makes each, more appropriate for specific environments and applications. Despite continuous enhancement of prosthetic devices, there are fundamental design



Figure 2.3 Commercially available myoelectric prostheses [19].

Table 2.1 Characteristics of commercially available prosthetic hands [19].

Hand and company name	i-Limb by touch bionics	Bebionic by RSL steeper	Michelangelo by ottobock
Weight	443-515 g	550-598 g	420 g
No of actuators	6 DC motors	5 DC motors	2 DC motors
No of DOFs	6	6	2
Active DOFs	F/E of MCP joint of each finger and thumb opposition	F/E of MCP joint of each finger	F/E of all the fingers contemporarily and thumb opposition
Passive DOFs	-	Thumb opposition (i.e., it is changed by the user)	-
Joint coupling mechanism	Tendon linking MCP to PIP	Linkage spanning MCP to PIP	Cam design with links to all fingers
Grasping configuration	Power, precision,lateral, hook, finger-point	Power, precision,lateral, hook, finger-point	Opposition, lateral, neutral mode
Maximum applied force	100-136 N	140 N	70 N

drawbacks in the state-of-the-art systems. Despite current drawbacks these prostheses are being commercially produced by different manufacturers , successful one are shown in Figure 2.3, with acceptable characteristics summarized in Figure 2.1. Body-powered prostheses are advantageous in terms of durability, training time, frequency of adjustment and feedback whereas myoelectric prostheses benefit from factors like cosmesis and are mostly used for light-intensity work. Body powered prostheses have kept the lead among users who do heavy work in harsh environments and are functionally minded with less regards for cosmesis [30]. However, users of myoelectric devices have improved psychosocial and social adaptation compared to users of body-powered prostheses [36]. According to Silcox et al. [35], the most recurring usage of myoelectric prostheses are social situations. Other superiority of body-powered prostheses are their durability, requiring less training and adjustments, being easier to clean and

keeping functionality even in the case of loose fit to the arm. Continued success of body-powered prostheses owes partially to device feedback in terms of improved interaction capabilities with objects [37]. Biddis et al. [38] concluded that consumer design priorities for body-powered prostheses include improved comfort, reduced mass, and further functional enhancements. They also referred to increased grasp force as one of the desires users seek in a prosthesis. Body-powered prostheses suffer from heat inconvenience, clothing damage, poor cosmesis and cable and harness maintenance issues. The most significant setbacks in myoelectric devices are related to prosthetic control. Financial issues are another factor in prosthesis choice. Externally powered upper-limb prostheses prices range from \$25,000 to \$75,000, considerably higher than their body-powered counterparts \$4,000 to \$10,000 [39].

Cosmetic passive hands are also able to deliver a direct mechanical feedback by assistance of a method called extended physiologic proprioception in which a human-machine interface is designed such that the body's physiological mechanisms are directly attached to the activation and sensing of the device being controlled [17]. In other words, user's natural proprioceptive feedback in a healthy joint is linked to the state of a prosthesis joint by coupling these two joints together through EPP [15].

An ideal prosthesis is not only able to detect physical interactions with its environment and sense the configurations like joint angles but it should also enable users to receive these information in an effortless manner [17]. There is a common belief that prostheses would have a better performance if they are controlled in a closed-loop manner; since amputees do not receive any feedback from their neural command there is no way to correct errors or deviations from desired path or force which makes the control architecture of these devices an open loop control. Provided that sensory path is intact users can benefit from both exteroceptive and proprioceptive information [41]. This hypothesis is based on the control process occurring in the sensory system of healthy persons which is illustrated in Figure 2.4. With body powered prostheses apparatus state and grip force sensing is achieved automatically through reaction forces transmitted to user's body. In this way no processing is required and sensing and actuating transducers are replaced by mechanical couplings.

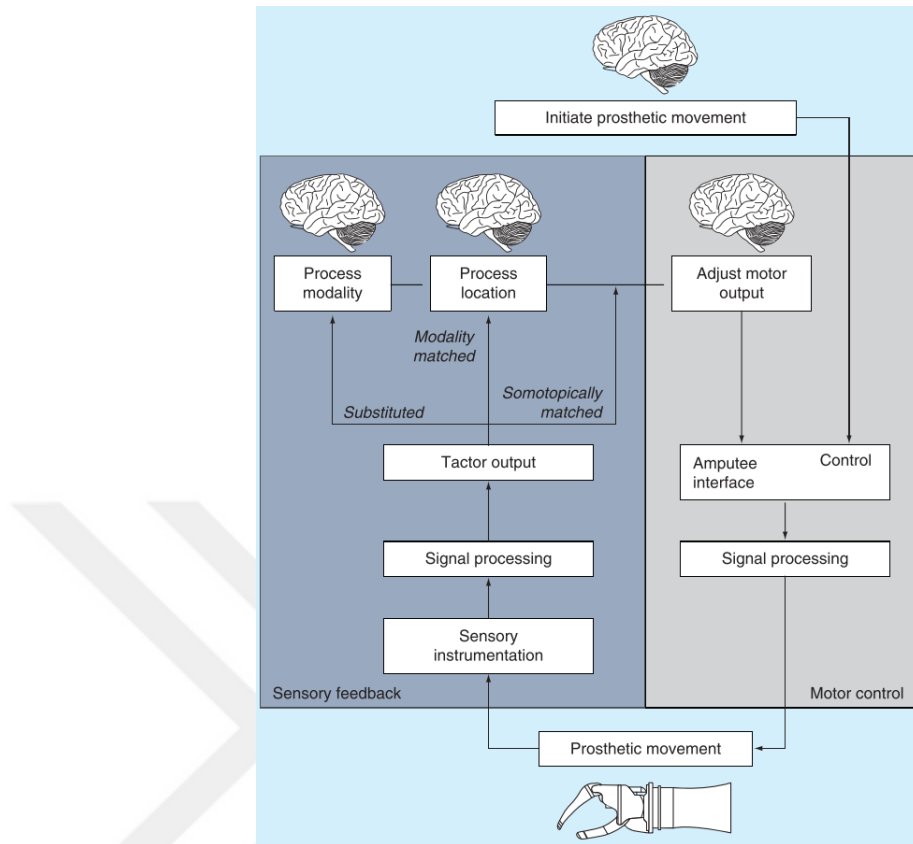


Figure 2.4 Control process of a myoelectric prosthesis with sensory feedback [40].

2.2. Proprioception

A normal hand is capable of managing to move in 27 degrees of freedom to perform functions which necessitates adjustment of strength as well as precise movement of hand[42]. As we grasp and manipulate objects with our hands, afferent tactile and proprioceptive signals carry information about different characteristics of the object including shape, size and texture of the objects and alert about slippage[43]. A range of cutaneous receptors convey information about skin deformation [44] and different receptors in the joints, muscles and skin convey information about the conformation and movements of the limb [45]. Proprioception is defined as the sensory perception and subsequent motor control of posture, balance, audiovisual-motor coordination and joint stability [46]. In simpler words it is the sense of relative position, velocity and kinesthetic force of neighboring parts of the body. Proprioceptive sense is derived from a group of afferent channels, including muscle spindles fibers, Golgi tendon organs,

joint angle sensors, and skin stretch (felt via cutaneous mechanoreceptors)[47, 48]. It is shown by Gandevia et al. [49] that efferent signals are also able to create a perception of arm movement even when it is stationary. Proprioception has been studied under different circumstances including anesthesia [50] and ischemia [51] as well as muscle vibration. However, the latter one distorts the proprioception rather than blocking it[52]. Despite knowing biological mechanisms which lie behind proprioception from a neurophysiological aspect there is not a consensus about how proprioception is coded in the central nervous system nor where or how it is processed in the cortex [14]. In a study by Srinivasan et al. [53] it is demonstrated that for discrimination of rigid surfaces both tactile and proprioception feedback is needed whereas for deformable objects tactile information suffices and proprioceptive information solely can not lead to desirable results. Gurari's research [14] confirmed this concept by designing a stiffness discrimination task.

Proprioception is sensed through a group of joint mechanoreceptors including: Ruffini Endings, Pacini Corpuscle and Golgi-like Receptors (a schematic representation is shown in Figure 2.5). Ruffini Endings are type of slowly adapting, low threshold receptor. They are found to react to axial loading and tensile strain in the ligament but not to perpendicular compressive forces. They are the prevalent mechanoreceptors in the wrist ligaments [54]. Pacini Corpuscle is a rapidly adapting, high threshold receptor responsive to joint acceleration and deceleration which is able to sense mechanical disturbances with a wide reception field [56]. Unlike Ruffini endings, these receptors are responsive to compressive forces not the tensile ones. They are the most abundant receptors in lateral ankle ligaments [57]. Golgi-like receptors are of the same family as the Ruffini endings, their effect is considered consequential in tracking tensile strain in the ligament, tendons of this type are inactive in immobile joint and begin to work at extremes of joint motions [58].

Proprioception is composed of a group of sensory information. Hughes et al. [59] classified proprioception into two modalities; joint position sense and sensation of limb movement. In their classification joint position sense is described as the ability of an individual to identify the static location of a body part. These senses are perceived

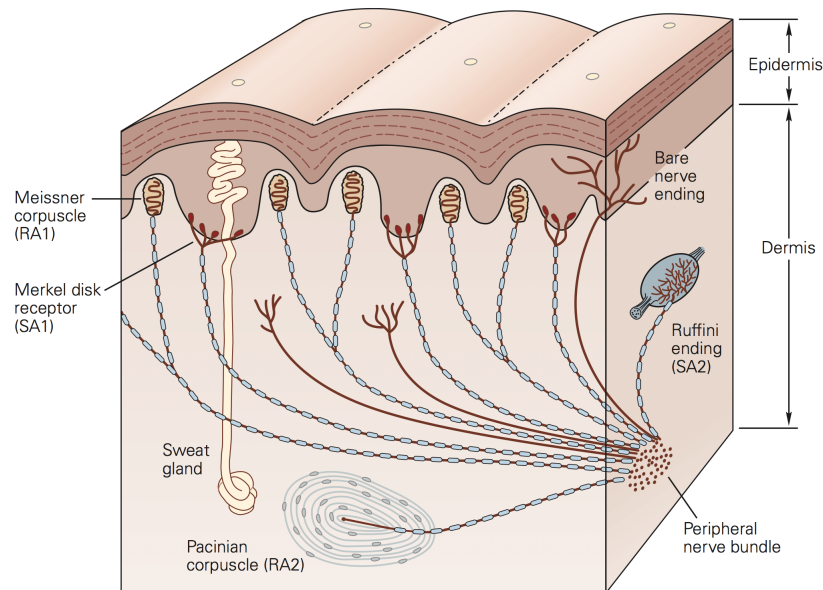


Figure 2.5 Mechanoreceptors in the skin [55].

by slowly adapting mechanoreceptors (primarily by secondary spindle endings and tendon organs in muscle). Conversely active motion sensing roots in more rapidly adapting mechanoreceptors including muscle spindle primary endings and lamellated corpuscles in other deep tissues. In a separate classification Hagert et al. [60] divided proprioception into three major senses composed of: kinesthesia, joint position sense and neuromuscular control which is a reflex control at the spinal cord and cerebellar level unlike the other two which occur consciously, illustrated in Figure 2.6. Their

logic relies on a study by Proske et al. [61] in which they postulated that although joint position sense and kinesthesia are both affected by action of muscle spindles their corresponding processing and interpretation areas in brain are separate. Kinesthesia is defined as the ability to sense both position and movement of both limbs and trunk. Skin receptors have been identified to be crucial in kinesthesia of finger joints due to the fact that muscles responsible for finger movements are located at a distance from the joint itself [48].

Proprioceptive deficits can be a result of sensory neuropathy conditions or surgery [62, 63]. Deficiencies in upper extremity proprioception have also been observed in normally aging adults [64, 65]. Evidence is available of proprioceptive impairments

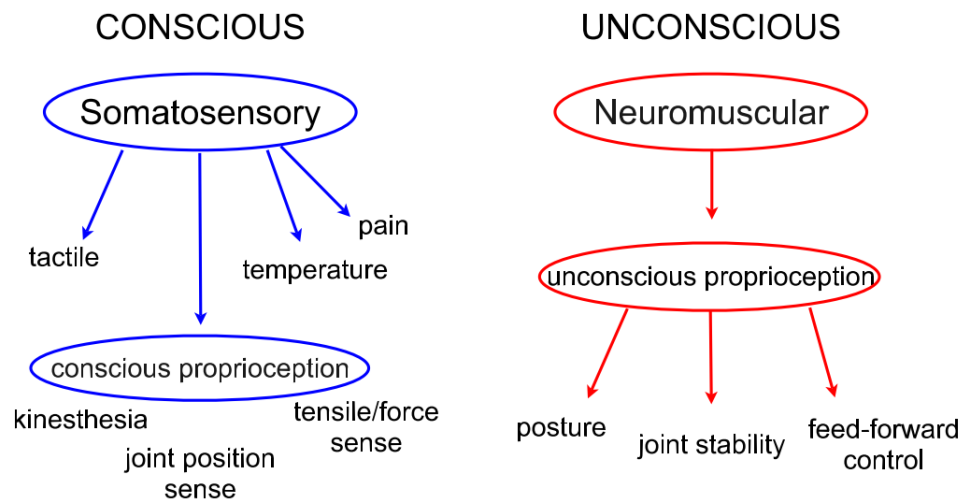


Figure 2.6 A schematic of various modalities of proprioception. Somatosensory senses are considered the conscious constituent of proprioception whereas neuromuscular control is carried out in unconscious level [60].

after stroke with lesions in thalamus posterior limb of the internal capsule (PLIC) and posterior parietal cortices (PPC) [59]. In patients with peripheral neuropathies that somatosensory is terminated along sensory path without any damage to motor commands, the reaching tasks are hindered due to lack of proprioception which results in deviated trajectories as can be seen in Figure 2.7 [66]. There are also evidence that patients with proprioception deficiency are not able to perform multi-joint movements which leads to impairment in interaction torques as a consequence of absence of proprioception [8]. Injuries to proprioceptive functioning can be as minor as damage to one of the sensation modalities like light touch or pressure to serious dysfunctions such as impairment to multiple or all modalities [67]. Multiple changes in peripheral nervous system have been mentioned in the literature associated with deterioration in proprioceptive function including increase in capsular thickness [68], decline in muscle spindle sensitivity [69] and diameter [70], and a lower total number of joint mechanoreceptors (especially for Ruffini, Pacinian and Golgo-tendon type receptors) and chain fibers [71]. Age related cognitive and sensorimotor processing ability are also considered to be a cause for changes in proprioceptive function [72]. Various researches studied the abundance of upper extremities proprioceptive impairment which concluded that it is equal or greater than rate of somatosensory dysfunction [73, 74].

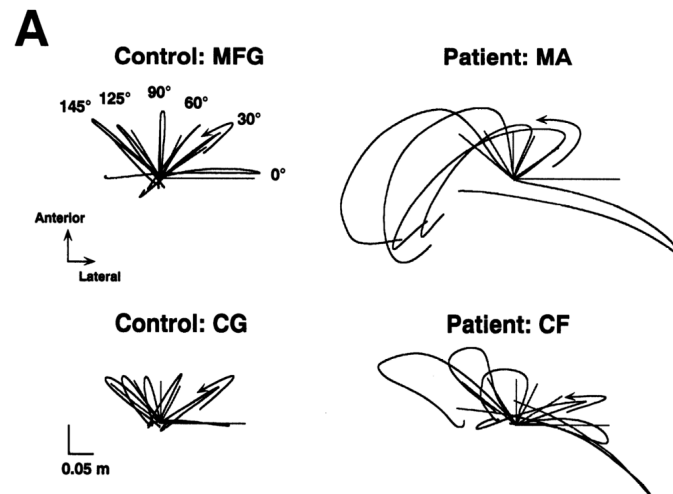


Figure 2.7 Hand path and reversal trajectory errors in healthy people (left) and deafferented patients (right) [8].

The advantageous fact about proprioception feedback is that it can be learnt, relearnt and enhanced by training. It was shown by Cho et al. [75] that stroke patients demonstrated significant improvement in their proprioceptive performance after certain period of training. One of the approaches to recreate proprioception is to reproduce naturalistic patterns of neuronal activation through Intracortical Microstimulation (ICMS). However, one of the obstacles in using this method is that electric stimulation of neuronal tissues do not yield in a naturalistic pattern; in fact, patients described its effects as ill-understood and difficult to predict. A rehabilitation method is called Reactive Muscle Activation (RMA) which has been proved to be effective [60]. It consists of a regiment of training which leads to reconstruction of unconscious activation of muscles to regain joint balance an example of an effective device is shown in Figure 2.8[60]. Passive sensory training is another solution for post-stroke rehabilitation which involves utilizing electrical stimulation to create activation of cutaneous nerves in the absence of muscle contraction. Conversely active sensory training includes a variety of exercises designed specially to train sensory functions [59]. The main issue with this kind of approach is that they require involvement of a therapist on a daily basis for as long as several weeks which necessitates a significant amount of human resources.



Figure 2.8 Powerball. The Powerball is a gyroscope that will apply a multidirectional inertia on the wrist muscles when activated. Its goal is to stimulate an unconscious proprioception rehabilitation through a reactive muscle activation.[60]

The sense of proprioception does not just encompass awareness of limb position, movement and neuromuscular control but plays role in a thorough conscious perception of self [60]. This sense of embodiment of body parts does not cease after an amputation. In fact many amputees express a sense of phantom limb, the feeling that missing limb is still there [76]. There have been studies in the literature which worked on the relation between this self attribution of a phantom limb and proprioceptive feedback [6].

There are several studies available in the literature in which effect of proprioception on successful manipulation of objects and possibility of implementation of artificial proprioception in prostheses application have been determined. Proprioceptive motion feedback was shown to increase success rate and ease of use in a positioning task. However, it decreased the movement speed (see Figure 2.9) [15]. What seems missing in the literature is a comparison between subjects' performance with natural proprioception and artificial proprioception [14].

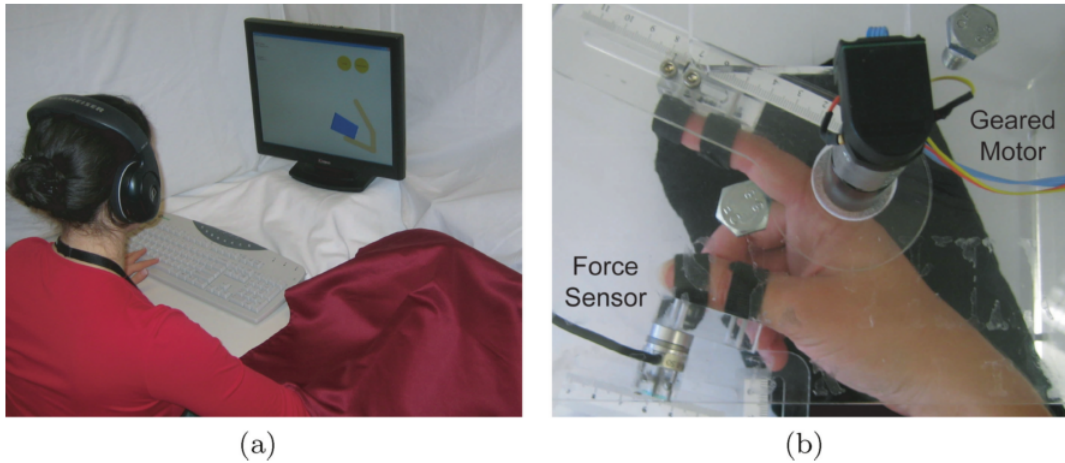


Figure 2.9 An example of artificial proprioception feedback in a grasping task. (a) Subject moves the virtual hand via force sensor and receives motion feedback via the designed haptic device (behind cloth) and a desktop computer. (b) Haptic device measures a grasping force input via the force sensor at the thumb to determine the movement of the virtual hand. [15]

2.3. Sensory Substitution

First attempts to take a methodological approach toward sensory substitution was made by Bach-y Rita in 1970s. He established employment of sensory substitution for research by designing a device named “Tactile Vision Sensory Substitution” (TVSS) from which visually-impaired users could benefit in tasks like recognizing large letters and catching a ball tossed at them [77]. The conventional configuration of providing sensory feedback can be illustrated by four cascaded blocks such in Figure 2.10; first neural signal should be received by a sensor and interpreted to its proper form in order to realize user’s intention, by converting these signals to an appropriate form of energy based on the designed delivering strategy user feels stimulation to become aware of his interactions [17]. Sensory feedback can be delivered to users in two ways; first

type is when sensory feedback is received in the same position that the real stimuli is initiated, the other method is called sensory substitution in which sensory feedback is delivered to another part of user’s body due to loss of sensory channel caused by

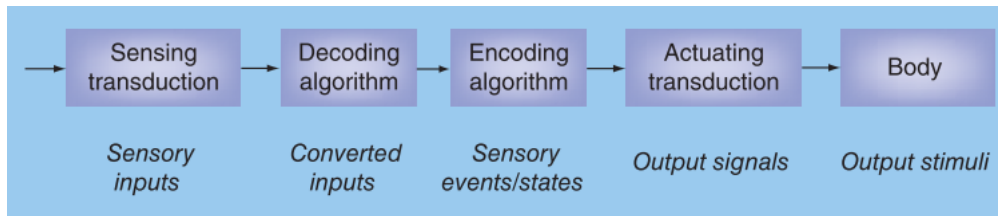


Figure 2.10 General layout for providing sensory feedback. In sensing transduction stage physical stimuli is converted from one form of energy to another which is more proper. Later a decoding algorithm identifies important sensory state components which will be used by an encoding algorithm to transform them into easily interpreting output signals. Eventually in the output stage obtained signal is converted to a form of energy to be applied on body sensory system.[17]

amputation or sensory deficiencies. The term modality-matched sensory substitution is used when the output stimulus is felt in the same modality as the sensory input for example, touch on the prosthetic hand is felt as touch. On the other hand sensory input can be mapped into another sensory modalities e.g. touch to vibration or force to stretch of the skin which is called modality-mismatched feedback. Theoretically it is easier to recreate modality-mismatched proprioception as there are multiple sensory channels and modalities available to feed the sensory stimuli. Additionally, modality-matched proprioception is intrinsically a more challenging task for engineers due to intrinsic characteristics of proprioceptions as well as loss of sensory channels because of amputation or sensory neuropathies [17].

An effectual feedback signal must produce the correct stimulus as well as guarantee that feedback signal is received as a cue rather than a distraction [40]. The main challenge in creating acceptable haptic feedback is generating a learnable sensory substitution experience for the user to attune to; since sensory path for receiving somatosensory feedback is no longer available, a satisfactory sensory substitution method seems necessary [78].

Physiological fMRI signals from late-blind subjects' brain has demonstrated noticeable activity in the visual object related area in comparing textures in regions related to both haptic perception and vision. [79]. Recent studies well established recruitment of visual cortex of visually-impaired individuals while processing either the spatial or the pitch properties of sounds carrying information in both domains (the same sounds were used in both tasks) [80]. In a study by Striem et al. [81] performance of congenitally blind users even outperformed the thresholds for World Health Organization (WHO) definition of blindness on Snellen acuity test utilizing a sensory substitution device (auditory feedback as visual cues) indicating that subjects are legally not functionally completely blind anymore. By having sufficient amount of training, prosthesis users may also learn to collect information about behavior of a haptic interface via sounds, vibrations and air currents produced by the device [31]. To reduce the requirement of visual feedback, experiments have been conducted with different strategies of delivering sensory feedback to the users, primarily by using miniature actuators positioned in contact with the skin [82]. Modality matched tactile stimulation seems necessary for conveying physiologically relevant touch feedback [6]. Current sensory substitution modalities can be classified in four main types; Vibrotactile feedback, Electrotactile feedback, Mechanotactile feedback and Auditorial feedback. Vibration is commonly a baseline standard with which other feedback methods are compared [40].

Vibrotactile stimulation is kindled by a mechanical vibration in the range of 10 to 500 Hz [32] and best results are when it is above 200 Hz. Main features of a vibrotactile stimulus are amplitude and frequency of vibration [83] although other features like pulse duration, shape and duty cycle can be modulated [17]. Frequency discrimination performance is the same for glabrous skin and hairy skin, however, at frequencies above 50 Hz stimulation frequency threshold of hairy skin decreases at higher frequencies [84]. According to a study by Stepp et al. [16] which aimed at comparing beneficence of amplitude modulation versus pulse train frequency for virtual object manipulation it has been concluded that amplitude modulation leads to more promising results in object manipulation. Other instances of vibrotactile feedback can be found in grip force information for prosthetic application [85], interaction force information in teleoperation assembly [86], and tissue interaction force information in

robot-assisted surgery [87]. Okamoto et al developed a tactile display in which they biased the perceived viscous and inertia properties of an object by vibration [88]. An example of vibrotactile feedback is shown in Figure 2.11. Moreover, augmentation of vibration feedback with force feedback reduced contact force error in a path tracking task [86]. The main limitation of vibrotactile sensory substitution is problems with conveying information about both amplitude and direction, although efforts have been made to deliver directional cue via asymmetric vibration [89]. Another disadvantage of vibrotactile feedback is its infeasibility in applications where there are rapid changes in applied forces such as teleoperation scenarios [90]. It can also cause irritation over long periods of operation [88]. Vibrotactile stimulation can trigger other senses as well, Roll et al. [92] realized that conveying a local vibration stimulus (between 40-80 Hz) over the tendons at the wrist of healthy subjects can produce a movement perception while the wrist is stationary.

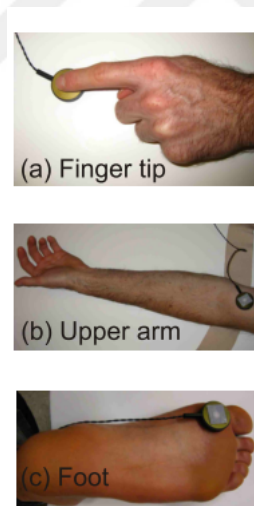


Figure 2.11 Vibrotactile feedback device. Here vibration feedback is delivered to subject in three ways; tactor can be placed under the finger(a), it can also be bandaged to subject's upper arm(b) alternatively it can be attached to ball of the foot [91].

Mechanotactile feedback is accomplished when a force normal or tangential to the skin is applied by a device to convey sensory information. This method is a popular approach in haptics as well, since it can carry rich amount of information of stimula-

tion. The main feature of this class of stimulators are accuracy (resemblance between input and output signals), precision, range, resolution, bandwidth and response time [17]. A variety of tasks have been experimented using mechanotactile feedback, in an object manipulation task, some improvement in amputee's performance was demonstrated incorporating mechanotactile feedback [93]. These systems have been shown to have superiority over vibrotactile feedback systems in terms of improved multisite force and spatial discrimination [94]. Like other methods there are drawbacks such as complex miniaturization, weight and energy consumption which obstruct usage of available haptic technologies in portable systems [17]. Comparing vibrotactile feedback with mechanotactile feedback, subjects discriminated better using mechanotactile devices, an example of a setup equipped with both of these feedback methods is shown in Figure 2.12 [95]. Additionally, another study compared mechanotactile feedback and vibrotactile feedback in which execution time of subjects were shorter with mechanotactile feedback [96].

Skin stretch is a submodality of mechanotactile feedback which has drawn a particular attention and is comparatively a new approach in sensory substitution field. Skin stretch has the benefit of projecting sensory information about both amplitude and direction simultaneously [90]. Integration of skin stretch to deliver proprioceptive feedback has been studied as well [97, 98]. Bark et al. [97] asked subjects to perform cursor movements using a single axis force sensor held between the fingers and thumb. Subjects demonstrated a better performance while receiving vibration/skin stretch feedback compared to no feedback condition. Subjects' results indicated a pattern of learning under sensory substitution feedback. In a similar study Wheeler et al. [98] utilized electromyographical signals from biceps and triceps of able-bodied subjects to control position and velocity of a beam to perform a positioning task. They realized that providing sensory substitution via skin stretch can elevate participants' results (decrease mean error) compared to those who performed the task with visual feedback. Sensory subtraction consists of substituting haptic stimuli, composed of kinesthetic component and skin deformation, with cutaneous stimuli only [99]. Meli et al. [99] utilized a 7-DOF bimanual teleoperation system to perform a peg and hole task which demonstrated that users performed better with sensory subtraction feedback compared

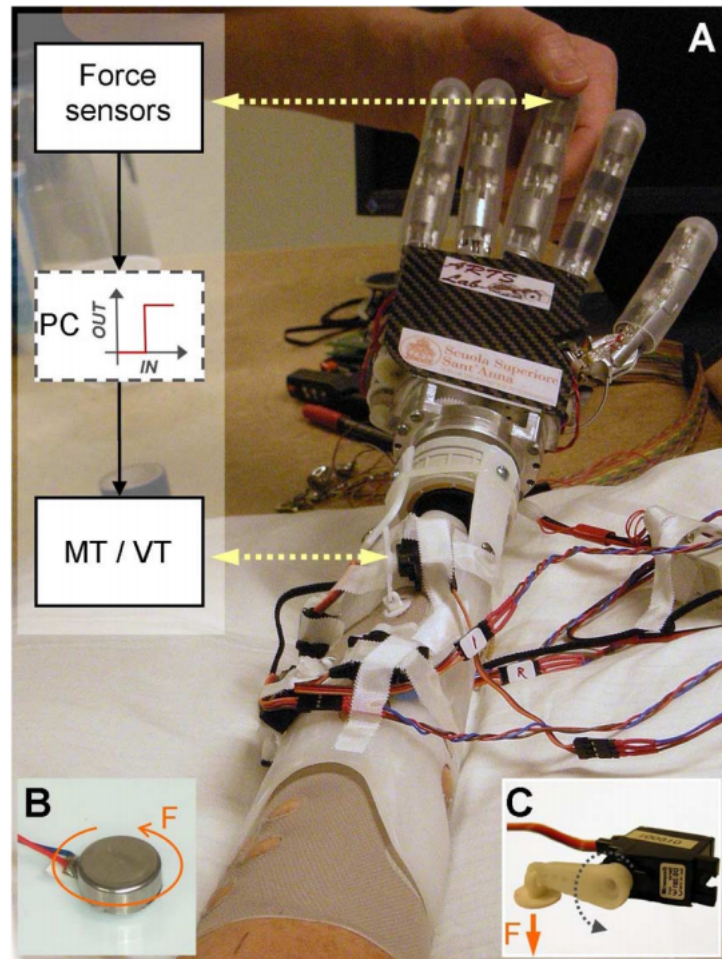


Figure 2.12 An example of a mechanotactile feedback haptic display. A. Experimental setup during mechanotactile experiments. B. Vibrotactile stimulator C. Mechanotactile stimulator; motor rotation is converted to a normal force on the skin [95].

to other two sensory substitution methods (cutaneous and kineasthetic feedback) although they performed worse when received complete haptic feedback, an example is shown in Figure 2.13. In a separate study, sensory subtraction was shown to be an intuitive sensory feedback in a stiffness discrimination task [100]. Guinan et al. [101] also used servo motors to carry a high friction surface across user's fingerpads to convey sense of translation and rotation for navigation purposes. Skin stretch feedback has also been used along with force feedback to bias the perception of friction of a virtual surface [102]. Augmentation of force feedback and skin stretch lead to less error in a needle penetration task [103].

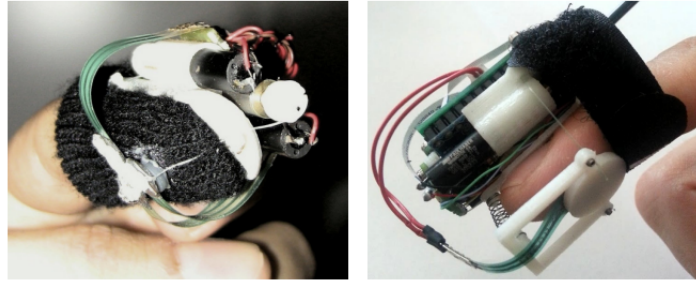


Figure 2.13 Mechanotactile feedback utilizing skin stretch method. fingertip skin deformation devices employed in sensory subtraction [99].

Electrotactile sensory substitution feedback benefits from certain advantages as well as suffering from disadvantages similar to other methods. In this method sensory substitution is normally achieved through modulation of electrical current parameters such as: amplitude, frequency and pulse rate to single or multiple electrode sites however, it can be designed to be either current- or voltage-regulated. The superiority of the former approach is consistency in current amount by modulation of tissue load whereas the latter one benefits from diminishing the danger of applying high voltage densities.

Currently modulation parameters include: current amplitude, pulse waveform, pulse frequency and duration and time span of pulse bursts. Electrotactile devices are dominant in terms of power consumption and response time compared to vibrotactile devices nonetheless they suffer from interference with myoelectric control systems when stimulation regions are near the EMG electrodes [17].

Auditory feedback is one of the most popular sensory substitution methods. Research studies provide evidence for a somatotopically-responsible region in the auditory cortex, indicating that an incorporation of sound and touch takes place there [104]. There are instances of application of auditory feedback in area of surgical robotics [105]. Auditory feedback has been implemented in applications such as conveying position of hand's digits and intended grasping pattern [106]. In a study by Gibson et al. [78] auditory feedback was employed to assist users of myoelectric gripper to adjust gripping force in a picking task (refer to Figure 2.14). It has also been evaluated to

convey visual cues to subjects, Eye music which is a recent example is described in

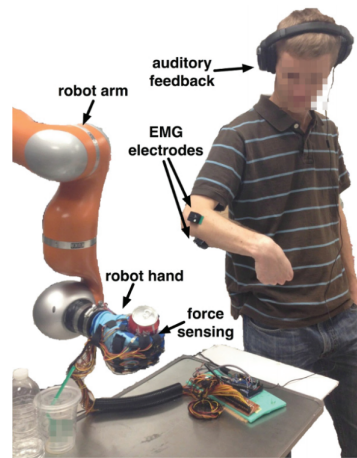


Figure 2.14 Auditory sensory feedback. Experimental setup in which the subject controls the robotic hand in grasping a soda can using myoelectric signals and auditory feedback to successfully adjust grasping force [78].

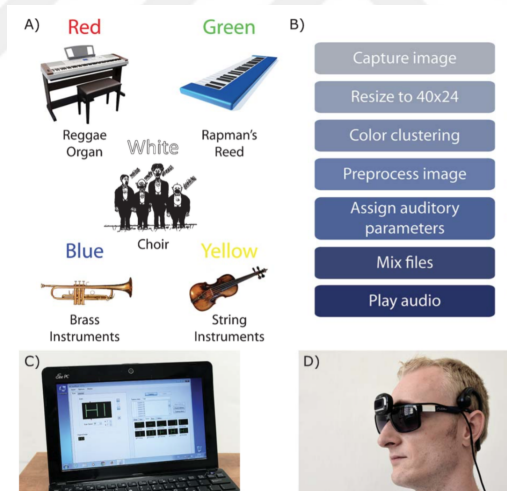


Figure 2.15 Concept, Algorithm and setup of an audio-visual sensory substitution system. A) Musical instrument used to represent color e.g. white is mapped to a choir and black to silence B) Visuo-auditory sensory substitution instances C) The EyeMusic application used on a laptop D) Sample setup equipped with camera on a sunglasses and earphones [107].

Figure 2.15. Drawbacks of auditory sensory feedback lie on training requirement for beneficial use, moreover, it enforces additional cognitive load to the user as auditory stimulation must be interpreted as tactile stimulation [40].

2.4. Virtual Reality for Prostheses and Rehabilitation

Virtual reality is a more appropriate method for proprioceptive rehabilitation since it simulates sensory responses similar to a real task [108]. Main aim of virtual reality systems is to first prevent from loss of sensory functioning and secondly facilitate an environment in which they can gain back their lost proprioceptive abilities in case of sensory deficiency. There are studies which have shown delivery of force feedback from interactions taking place in a virtual environment improves performance and dexterity and helps subjects operate faster [109]. In another study by Brown et al. [110] they simulated two nonlinear virtual springs under different feedback conditions and asked subjects to adjust non-linearity of two springs until the difference is not distinguishable; subjects performed better in conditions in which sensory substitution was collocated. (input force and related sensory substitution feedback was delivered in the vicinity of each other.)

Engaging games are the underlying component of many robotic rehabilitation devices. These games are not only beneficial for patient's motivation and retention but also enable him to compensate for proprioceptive deficits by relying on his visual feedback [59]. Among the empirical studies we can mention the virtual reality developed in Italian Institute of Technology which forces patients to rely on their proprioception [111, 112]. Gurari et al. [91] also conducted a study on effect of proprioceptive motion feedback in unimpaired subjects in a stiffness discrimination task. In [15] they considered contribution of proprioceptive feedback on successful manipulation of a virtual prosthesis using a virtual environment equipped with admittance control. For training intentions, virtual simulation can supply the user with a realistic and configurable environment where all types of scenes can be recreated and repeated. Applications of virtual reality in haptics is as popular as in robotics and medical training. Strong point of these systems lies in their objective assessment and effective rehabilitation training which owe to their ability to allow user confirm his own movement without therapist assistance as well as being able to view the results of the training in the near real time [75]. Two basic methods are present for simulating physical part behavior; physically based modeling (PBM) and constraint based modeling (CBM); PBM utilizes

System	Year	Assembly method	Key Features	Haptic Device
HIDRA[16]	2001	Collision detection	Integrates a haptic feedback into a (dis) assembly simulation environment Manipulate parts using two fingers	Phantom desktop
MIVAS [10]	2004	Physics based	Optimization techniques for complex models and assembly operations Tracking of user movements and voice commands Realistic virtual hand interaction for grasping of virtual parts Documentation of assembly planning results	CyberGrasp one hand
VADE [12]	2004	Physics and constraints	Users can perform the assembly using hands and tools such as screw drivers During the assembly process VADE maintains a link with the CAD system Let the user to make decision and design changes Swept volume generation and trajectory editing	CyberGlove two handed
SHARP [11]	2006	Physics based	Capability of create subassemblies Swept volumes for maintainability Network module for communication with different VR systems Portable, runs on different VR systems such as HMD, CAVE, projection walls and monitors	Phantom omni dual handed
VEDAP-II [7]	2009	Physics based	Oriented to assembly planning and evaluation Focuses on modeling the dynamic behavior of parts during virtual assembly operation	CyberGrasp one hand
MRA [21]	2009	Physics based	Use of low cost technologies for two hands assembly Real scale projection and tracking system to change point of view The system demonstrates the assembly procedures and the user must repeat it	6D35-45 / Wii-mote
VCG [3]	2010	Constraint based	Oriented to assembly planning and training Method of constraint guidance to perform the assembly Use of virtual fixtures, use of mechanical constraints, intuitive assembly, on-line activation of kinematic constraints	Virtuose 6D35-45 one hand
IMA-VR [5]	2010	Constraint based	Virtual training system for the cognitive and motor skills transfer combining haptic, gestures and visual feedback Uses the concept of spring-damper model to avoid parts interpenetration Visual dynamic behavior of parts to represent manipulation of real parts	Phantom/ LHIFAM/ GRAB two hands
HITsphere system [6]	2011	Physics and constraints	Immersive virtual environment with walking capability to simulate ground walking Free manipulation of virtual objects Automatic data integration interface Constraint-based data model is rebuilt to construct the virtual assembly environment	Phantom Premium one hand

Figure 2.16 Examples of virtual reality systems in haptics [113].

Newtonian physics to describe motion and forces and to model physical behavior in virtual environment while CBM employs geometric constraints to locate the parts in the assembly position via decreasing the degree of freedom of manipulated part [113]. Instances of usage of virtual reality systems for rehabilitation and sensory substitution feedback purposes are studied in the literature which will be discussed in detail. Figure 2.16 represents a review of the softwares developed for haptic applications.

Virtual training holds the second place among all the alternatives in terms of user preference; where first place belongs to master-apprentice training [114]. Immersive training demonstrated to enhance performance on the real task compared to conventional 2D instructions [115]. Virtual tasks generally take longer compared to real one however it is shown that although participants performed slower three-folded in virtual training, they performed three times faster in the real assembly test compared to ones who were trained with physical puzzles, an example of a puzzle solving application is shown in operation in Figure 2.17 [116]. Some of the factors which contribute to this difference are; the manipulation interface used (mouse, glove, haptic



Figure 2.17 pretesting assembly environment mode of SPARTA in a puzzle assembly task.[116]

device, etc), the physics simulation performance, the manipulability of virtual objects, the shape and weight of virtual objects, the camera manipulation, the rendering type and force feedback [113]. Williams et al. [117] built a simulator in which the spine can be explored and manipulated with index fingers.

There are almost three main constituents present in any virtual reality software; Visual components, Mechanical feedback (physical components) and haptic feedback component. There are three principal softwares available to develop virtual reality environments in haptics and medical training; CHAI3D, SOFA simulation framework and SPARTA.

CHAI3D is an open-source, multi-platform C++ library which enables designer to employ both haptic and visual rendering of an object to create real-time simulations. CHAI3D supports different commercially available haptic devices and algorithms that can be used or extended such as graphic and haptic rendering, collision detection, file support, timers and extensions [118]. Two modules are available for any object including GEL and ODE; GEL class is employed to simulate deformable objects while ODE is applied to replicate rigid objects. A significant amount of research conducted, relied on CHAI3D [16, 99, 118–120]. An example is demonstrated in Figure 2.18.

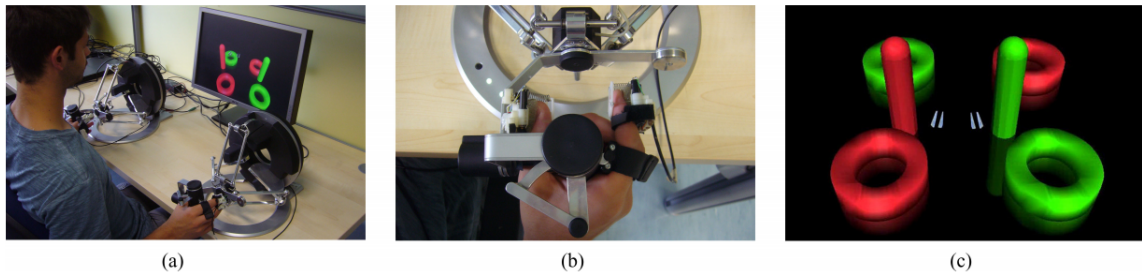


Figure 2.18 Experimental setup. Two cutaneous devices had to be worn by subjects on each hand, they let users control pliers via multiple Omega7 devices. (a) General overview of setup. (b) Detail of one hand wearing the devices. (c) Virtual environment with surgical pliers [99].

SOFA (Simulation Open Framework Architecture), which is based on Finite Element analysis, mainly aims at real-time simulation with an emphasis on medical simulation. Graphic Processing Unit (GPU) can be used to assure real-time computation of complex deformable models with nonlinear geometry using implicit and explicit methods [121]. SOFA can be implemented in complex scenes as cardiac surgeries (as shown in Figure 2.19) as well as haptic applications. It is worth to mention that geometry and boundary conditions are important aspects for finite element simulation. In a study by Talbot et al. [122] instances of training, planning and guidance applications are presented. SOFA was evaluated by seven cardiologists and was rated 2.5 out of 3 which appears to be a promising result. SPARTA (Scriptable Platform

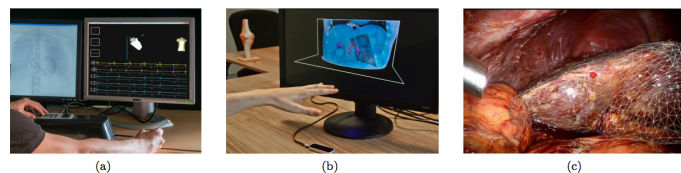


Figure 2.19 Simulation implementation in SOFA. (a) Virtual training in cardiac electrophysiology, (b) patient-specific planning of cryosurgery (c) intra-operative guidance for laparoscopy [122].

for Advanced Research in Teaching and Assembly) merges VRJuggler for stereoscopic immersion, OpenSceneGraph for graphics, VoxmapPointShell (VPS) for physics of collision between virtual objects, and VRJuggLua, which enables creating scenes and objects rapidly utilizing the Lua scripting language [116].

3. METHODOLOGY

Proprioceptive feedback for the users of robotic prostheses is still one of the challenges in the field of haptics. Since sensory receptors are not available anymore, recreation of this sense is a complex task. Although efforts have been made to recollect the lost data through available devices, mainly prostheses, and to explore for a solution to deliver this information to subjects there is a lot to be explored. The main challenge here lies in the nature of proprioception which is perceived and interpreted in a complicated process. Bringing back this perception requires a broad knowledge about mechanism behind proprioception and mechanical procedures available. Since conveying physiological proprioceptive feedback is impossible in a non-invasive manner, the main focus in this field is on sensory substitution of proprioception which is usually referred as artificial proprioception. Although there have been several studies on artificial proprioceptive feedback [15, 91, 123], they mostly focused on a single DOF task or limited their tasks to targeting task which requires merely a coordination of position [14, 31]. However, an important aspect of proprioception is kinesthesia which includes comprehension and interpretation of internal and external forces applied to different parts of a limb [124].

Our ultimate goal is to identify contributions of sensory substitution of position and force feedback on coordinated manipulations in multi-DOF, therefore, we have designed and developed a new experimental setup and a methodology. The proposed methodology is based on an unstable task called “Strength-Dexterity Test” designed by Valero et al. [12] to evaluate human control ability in a dynamic task. In this test, subjects are asked to compress a spring up to buckling. We have implemented a virtual model of this test. The experimental setup consists of a novel 2-DOF haptic interface, a 2-DOF input device, a 6-DOF force sensor and a virtual environment.

3.1. Experimental Setup

The main component of our experimental setup is the haptic device which will be elaborated in Ch.4. The input device, two Arduino Mega 2560 boards, an ATI force sensor F/T Sensor Nano17, vibration motors and a virtual reality environment are additional components of our setup. Specifications and functionalities of the latter one will be discussed in the Virtual Environment section and the former ones appear in the Hardware section.

3.1.1. Hardware

The haptic device and the input device have been designed to interface with the index finger and their degrees of freedom are translation along Y axis and rotation around Z axis. Their workspace and output capabilities have been specified based on the human finger capabilities. Our workspace with corresponding axes are shown in Figure 3.1 .

An Arduino Mega was used to perform control algorithms and electrical commands. The Arduino Mega operates with ATmega1280 microcontroller with 54 digital i/o pins, 16 analog inputs, 4 UARTs (hardware serial ports), a 16 MHz crystal oscillator, a USB connection, a power jack, an ICSP header, and a reset button. Operating voltage is between 6-12 V and each pin is able to provide 40mA. It is worth to mention that only one of the serial ports is connected to the USB connection of the board. Other serial ports can be connected to peripheral devices upon request via an FTDI cable.

There are also 6 Interrupt pins available which suit reading digital encoders. The board is capable of providing 5 Volts and 40 mA on each pin.

The input device is comprised of two encoders (OMRON E6B2), a brushed DC motor (Mitsumi Motor RS-540SH), a thimble and four MicroDrives 12-mm vibration motors (refer to Figure 3.2, Left). This 2-DOF device is kinematically analogous to

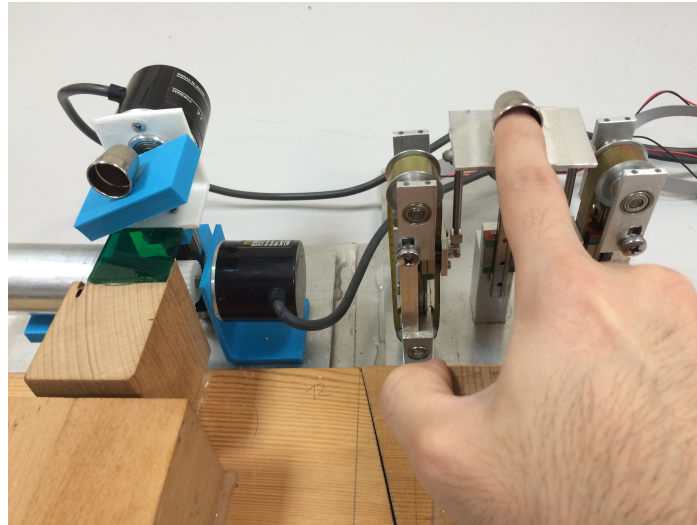


Figure 3.1 Input device (left) and haptic interface (right).

the haptic interface with the only difference that translation and rotation movements are decoupled which resulted in considerably less friction. The encoders are used to measure finger displacement; one for translational movement of the thimble and the second one for measuring orientation of the thimble. A pinion-and-rack mechanism guided on a linear rail is used to convert translation into rotation for measurement purposes. A general image of the setup is shown in Figure 3.1. Weight and friction of the device were compensated with the motor operating at a constant current.

In order to give vibration feedback to subjects we used two coin vibration motors. F/T ATI force sensor is used in our application which measures forces and torques in 6-DOF (shown in Figure 3.3). Force sensor is connected to PC via a NI PCIe-6363 Data Acquisition card. Three LED lights were also employed to give subjects visual cues about different status of the task. A green LED indicating trial beginning, a red LED indicating arrival to the goal position and a yellow LED for task completion.

Vibration feedback was delivered to subjects using the method proposed by Cipriani et al. [83]. Each vibration motor is composed of an electrical motor with mass M with a rotating eccentric mass m deployed on a shaft and bearing; the rotation of unbalanced shaft generates a forced vibration with the angular velocity ω , amplitude A which is proportional to weight of eccentric mass m to its eccentricity e . In this

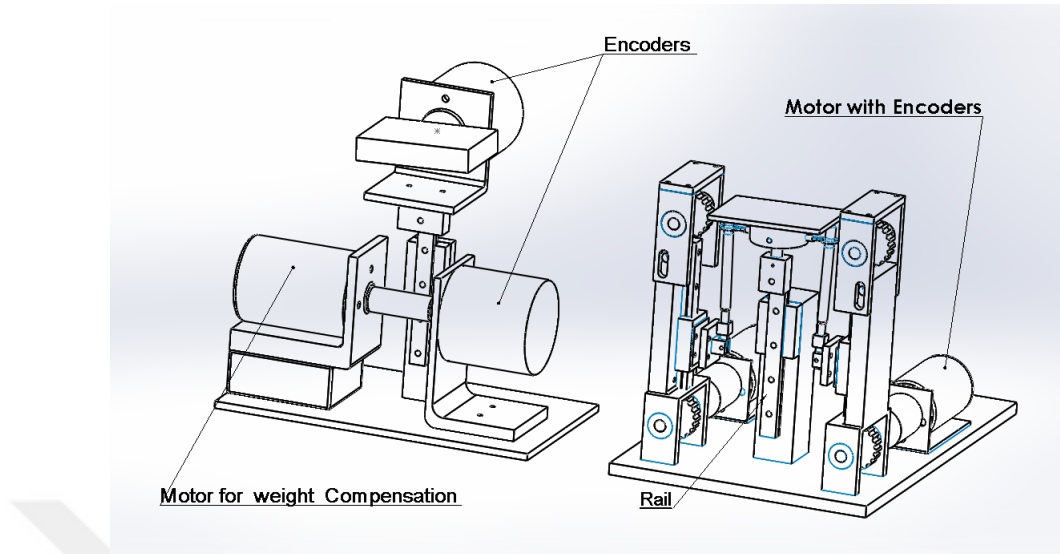


Figure 3.2 General design of haptic device (right), and input device (left).

representation generated force can be modeled as:

$$F = (m.e.\omega^2)\sin(\omega t) = A\sin(\omega t) \quad (3.1)$$

A two-tone combination (with two vibrating motors) with constant amplitude and by neglecting phase shifts yields:

$$\begin{aligned} \sin(\omega_1 t) + \sin(\omega_2 t) &= 2\cos\left(\frac{\omega_1 - \omega_2}{2}t\right)\sin\left(\frac{\omega_1 + \omega_2}{2}t\right) \\ &= 2\cos(\omega_{LF}t)\sin(\omega_M t) \end{aligned} \quad (3.2)$$

Where:

ω_{LF} (lower frequency tone) : half the difference between ω_1 and ω_2

ω_M : mean angular speed value

Provided that a minimal difference exists between frequencies this interface is called *beat*. On the condition that amplitude and angular speed are fixed, we have:

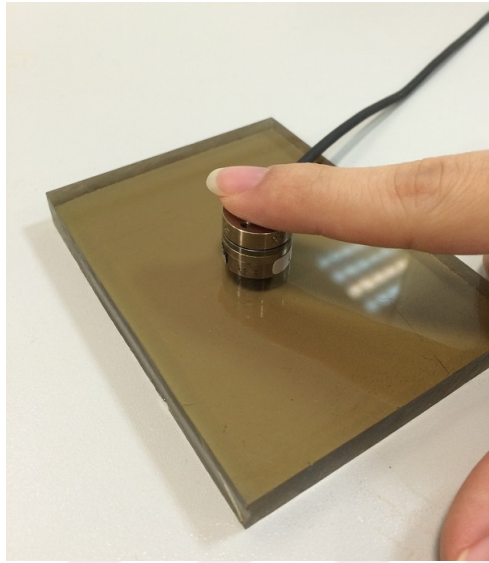


Figure 3.3 Force sensor ATI Nano-17 used as an isometric input device.

$$\sin(\omega t) + \sin(\omega t + \phi) = 2\cos\left(\frac{\phi}{2}\right)\sin\left(\omega t + \frac{\phi}{2}\right) \quad (3.3)$$

if the phase shift is almost zero $\phi \approx 0$ the waveform has an amplitude as twice as the original waveform called *constructive interference* while if the cosine phrase is equal to $\pm\pi/2$ the output becomes zero which is called destructive interference.

It is shown in Figure 3.4 that when motors are placed coaxially vibration of each motor is combined constructively which avoids interference caused by slight differences in frequencies. Hence, despite rotational frequency difference the rotors are always magnetically synchronised which results in a greater amplitude and a distinctive frequency component[83]. In this study we decided to utilize an envelop signal which was constructed by two motors mounted coaxially on the skin. Motors were powered with PWM signals which were 11% different from each other in terms of dutycycle; this lead to wave forms which contained frequency characteristics of both vibrations, as can be seen in Figure 3.5. Subjects described vibration feedback to be distinctive and distinguishable from each other.

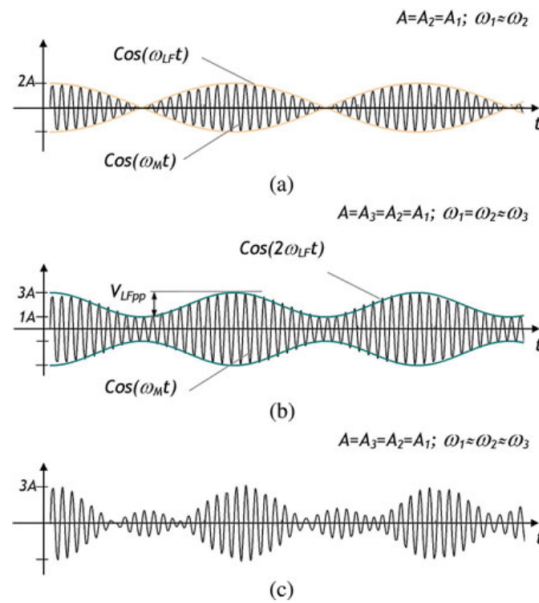


Figure 3.4 Combination of multiple sinusoidal waves in time domain. (a) Beat. combination of two waves with equal amplitude A and different frequencies ω_1 and ω_2 results in a sinusoid with angular speed ω_M which is equal to the average between ω_1 and ω_2 , and an amplitude of $2A$ which is modulated by a sine having angular speed ω_{LF} half the difference between ω_1 and ω_2 . (b) Sum of three vibrations, two of which similar and the third with equal amplitude but different angular speed. This time the envelope modulates at twice ω_{LF} . (c) Sum of three vibrations with equal amplitude but different frequencies: all combinations of frequencies contribute to the output waveform [83].

3.1.2. Virtual Environment

To develop the virtual environment of the experimental setup, our first attempt was to design our scene in CHAI3D which is a popular library for developing haptic virtual environments. In order to achieve this goal we modified an existing example of CHAI3D; Membrane since this example suited our purpose the best. Membrane scene consists of a deformable plate which can vibrate by applying force. The ball which is the controllable component of the scene is guided either by PC mouse or a haptic device. Our first step was to design a deformable spring by allocating certain amount of stiffness to the virtual springs which hold these components beside each other so

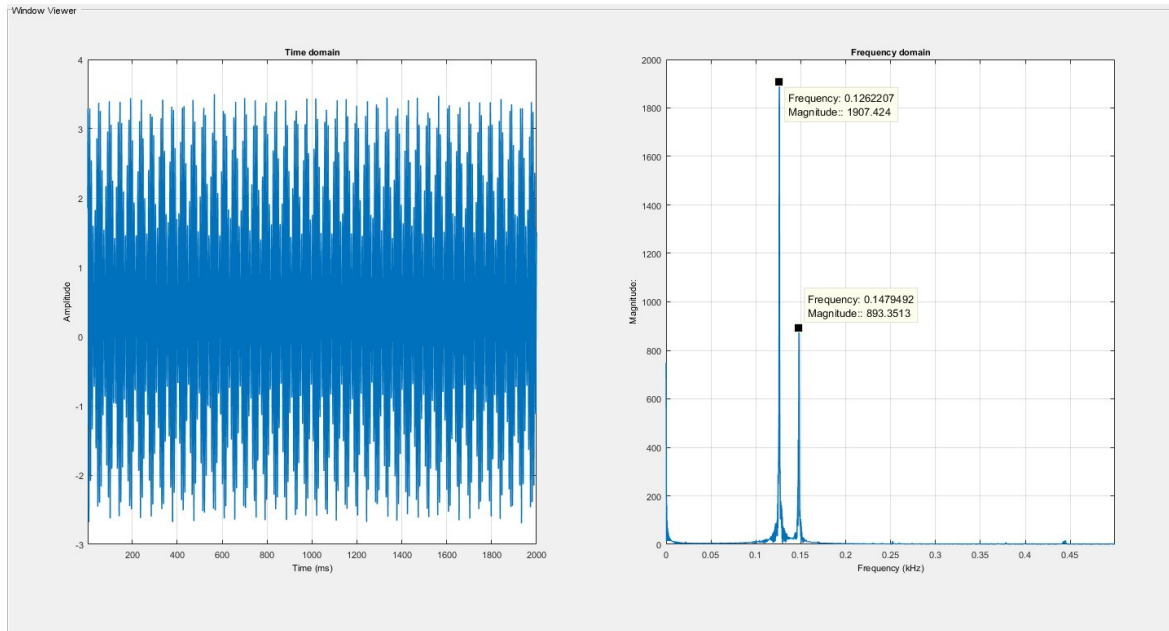


Figure 3.5 Time domain measurement and frequency content of a vibration actuation with duty cycle of 63% and 74%.

that a spring behavior can be obtained. CHAI3D examples are divided to two general groups of GEL and ODE; it means a scene should represent either a rigid body or a deformable object. However, our application necessitated existence of both these types in the scene (a deformable spring and a rigid spring cap) which made the task challenging. Having gone through the documents available online and asking experts of the field including Dr. Sonny Chan in Salisbury Robotic Lab who released the new version of CHAI3D library we concluded that our intended aim can not be achieved by CHAI3D. Consequently, alternative programs were searched.

After discussing the issue with researchers in the community we concluded that SOFA could meet our expectations. Therefore, we used SOFA 15.12.0 for our application. SOFA installation steps can be described as follow. Raw codes downloaded from GitHub are compiler-independent. Since we need to work with Visual Studio, the codes must be structured in a way that can be interpreted by C++ coding logic language. To perform this task CMake is needed which converts compiler-independent codes to a code which is comprehensible by a C++ compiler software. Next step was to build the C++ comprehensible codes with Visual Studio 2012. After compiling the scripts, SOFA was ready to work with. An advantageous point about SOFA is that it allows

users to operate with the system either through a GUI environment or directly through Visual Studio by composing your own scene from scratch. We decided to work with the GUI environment as it was more convenient and less complicated. SOFA components are modeled using a dynamic or quasi-static system of particles. The node coordinates are the independent DOFs of the object, and they are governed by equations of the following type:

$$a = PM^{-1} \sum_i f_i(x, v) \quad (3.4)$$

Where:

x: Position vector

v: Velocity vector

f_i : Different force functions

M: Mass matrix

P: Projection matrix to enforce boundary conditions and displacements

a: Acceleration of the object

SOFA GUI is composed of node blocks including mechanical property, force field, constraint and mapping blocks etc. All these nodes are added as subgroup of “root”. There is a hierarchical order among nodes i.e. higher nodes have control over the lower ones. Each object in the scene is a combination of three models; visual model, internal model (mechanical model) and collision model. Lacking any of these models makes the object an incomplete model which is short of either appropriate visual representation or does not react against external forces. To enforce consistency in a scene one of these models acts as the master which imposes its displacements to slaves using mappings. Let \mathcal{F} be the function to map position x_m of the master to the model position x_s of the slave. Then we can write:

$$x_s = \mathcal{F}(x_m) \quad (3.5)$$

and the velocities are mapped in the similar way:

$$v_s = Jv_m \quad (3.6)$$

in which Jacobian matrix $J = \frac{\partial x_s}{\partial x_m}$ relates master and slave velocities. Accelerations

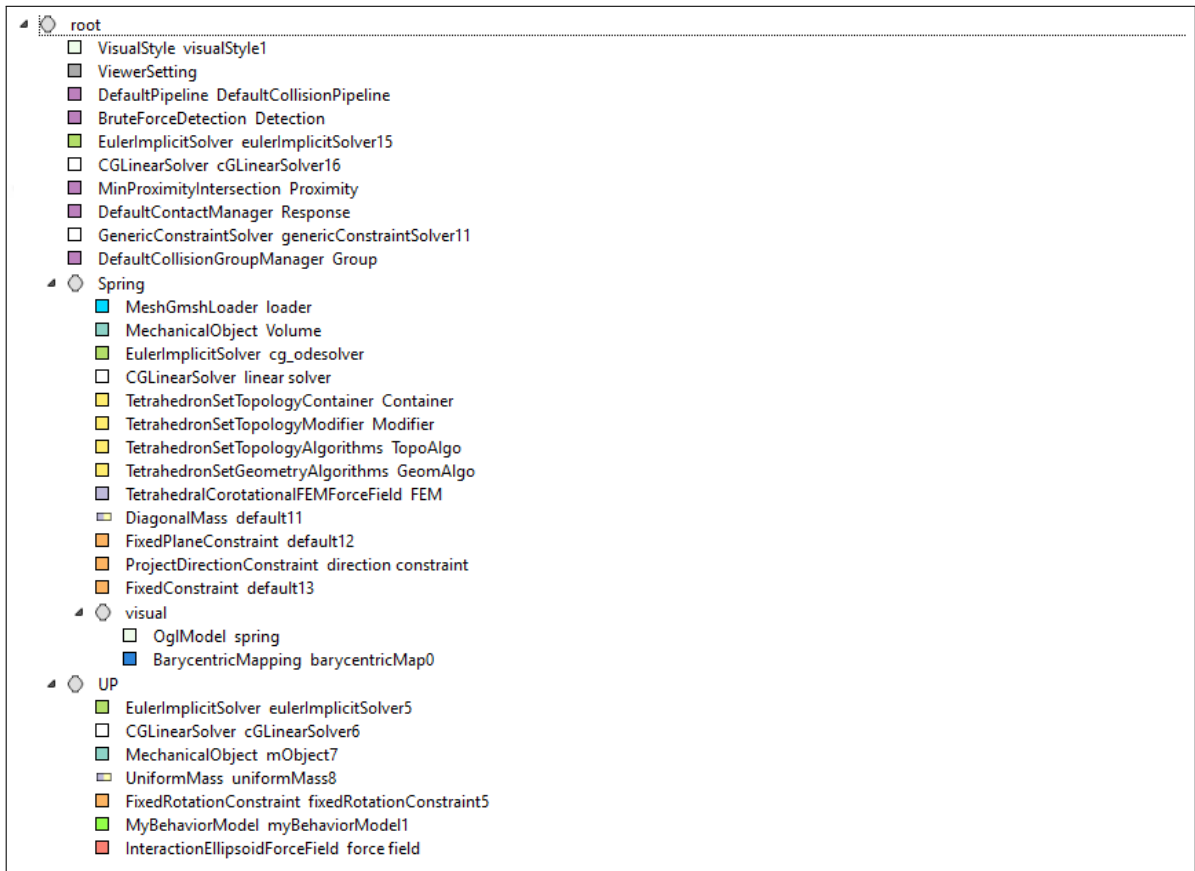


Figure 3.6 Hierarchical representation of our developed virtual reality model.

can be mapped using:

$$a_s = Ja_m + \frac{\partial J}{\partial x_m}v_m \quad (3.7)$$

Resulting SOFA scene with corresponding components are shown in Figure 3.6. Each of the employed components and its functionality in the scene is explained in Table. 3.1.

Table 3.1 SOFA components

Component Name	Functionality
VisualStyle	Adds the graphical settings to execution window of the program.
ViewerSetting	Facilitates modification of the configuration for the viewer of the application.
DefaultPipeline	Manages the default collision detection and modeling pipeline.
BruteForceDetection	Calculations regarding collision detection using extensive pair-wise tests.
EulerImplicitSolver	Implements the logic of time integration using backward Euler scheme.
CGLinearSolver	Is a linear system solver using the conjugate gradient iterative algorithm.
MiniProximityIntersection	Is composed of a set of methods to compute if two primitives are close enough to consider them collided.
DefaultContactManager	It is a default class to create reactions to collisions.
GenericConstraintSolver	Employing the linear complementary problem formulation to solve constraint based components.
DefaultCollisionGroupMManager	Responsible for gathering colliding objects in the same group for consistent time integration.
Spring	Contains all the components implemented to replicate the virtual spring.
MeshGmshLoader	Used to read the topology and the geometry from a file.
MechanicalObject	Involves all parameters concerning MechanicalState such as visibility of different components of the mechanical object, position shift or scale etc.
TetraHedronSetTopologyContainer	The tetrahedral connectivity is stored in it.
TetraHedronSetTopologyModifier	Modifies the topology by adding and removing tetrahedra.
TetraHedronSetTopologyAlgorithms	Creates and manages algorithms to keep the integrity of mechanical object which is implemented in two aspects of the mechanical object; topologically and geometrically.
TetraHedraCorotationalFEMForceField	Allows for large displacements or rotations in the model, while relying on a linear expression of the stress-strain relationship.
DiagonalMass	Defines specific mass for each particle.
FixedPlaneConstraint	Projects particles on a given plane and forces them to keep their location in the plane.
ProjectDirectionConstraint	Attaches given particles to their initial positions.
FixedConstraint	Implements the product with matrix P to cancel the displacements of the particles depicted in squares in the figure.
Visual	Represents the visual modeling of the spring.
OglModel	Reates the generic visual model for OpenGL display.
BarycentricMapping	Performs the mapping from mechanical model to the visual model so that the model behaves consistently.
UniformMass	Uses barycentric coordinates of the child (visual model) with respect to cells of its parent (mechanical model).
UP	Constitutes the mass or the end effector which interacts with the spring.
FixedRotationConstraint	Prevents rotation around X/Y/Z or a combination of them. It is utilized to prevent the end effector to rotate or slip away from the spring end.
MyBehaviorModel	Component which connects the end effector to the robot.
InteractionEllipsoidForceField	Arepulsion force applied by an ellipsoid toward the exterior the interior. This node is employed to cancel the weight of the end effector.

To transfer encoder readings of motors from Arduino to SOFA each encoder reading was sent to a serial port of Arduino to be transferred to PC via USB connection. There are two approaches for sending serial data via serial port; either sending them as ASCII characters or sending them as one byte of data. Since reading ASCII characters requires a conversion from ASCII codes to corresponding numerical value it demands extra computational and programming processing which is not desirable. However, by dispatching data in byte we avoid these complications. Since the data received from USB is in byte form, conversion from byte to number is executed automatically. Hence, we decided to send data in byte form. Each component of data on individual serial line of Arduino was separated to high byte and low byte employing *highByte* and *lowBytes* functions of Arduino. In this manner we were able to transfer numbers greater than 255 since each byte can contain a value between 1 to 256. In the case that position or rotation values are greater than 256 the number is divided to 256 where high byte is the quotient and low byte is the remainder of division. Due to some synchronization issues data was sent to PC via Sparkfun FTDI cable with connecting Rx and Tx pins of Arduino to FTDI cable. Each USB connection is detected as a COM (Communication) port in Windows. Therefore to get access to the data from Windows the same COM port had to be opened in SOFA. A code was generated to open the corresponding COM port in C++ and timing parameters were adjusted so that there will not be any asynchron between sent data and received data. Later, data was scaled to correspond to an acceptable value of workspace in SOFA.

Next step was to connect force sensor to SOFA. As we were using NI-DAQ card to read the force sensor values, we utilized NI-DAQmx library developed for programming in C++ environment by National Instrument. First step in putting the codes in service was to import NI-DAQmx library as well as main function definitions and headers required for running the program into SOFA. To accomplish this task we added these codes to CMakeList file which is responsible for compiling the C++ dependent code in CMake. Since the force sensor converts mechanical forces to electrical voltages, the obtained values from the force sensor had to be converted to their corresponding force values. A calibration is performed to represent the correct value in Newton. Consequently, we derived the calibration matrix from ATIDAQFT.NET program provided

by the manufacturing company of the force sensor. Since the device measures applied forces and torques in 6 degrees of freedom, obtained calibration matrix was a 6-by-6 matrix. Similar scaling procedure was carried out to convert force readings to their corresponding visual values in SOFA. Force sensor was set to measure data in 1 kHz. By integrating all these parts together, we managed to reach our aim which was developing a virtual reality system reflecting mechanical movements into a visual movement in virtual environment. Obtained scene is shown in Figure 3.7.

3.1.3. Buckling Model

Cuevas et al.[5] modeled the overall one dimensional dynamics of the compression spring buckling system as a subcritical pitchfork bifurcation of the endcap angle θ projected onto its first principal component F_s . Derived formula can be described as:

$$\dot{\theta} = \alpha(F_s - F_{max})\theta + \beta\theta^3 - \gamma\theta^5 \quad (3.8)$$

Where α, β and γ are scaling parameters, F_s represents compressive spring force, $\dot{\theta}$ is the angle change rate (angular velocity) and F_{max} represents the maximum attainable compressive spring force. For our simulation we considered a compression spring with design specifications; free length=76.2 mm, mean diameter=8.7 mm, wire diameter=0.79 mm, total coils=24, material: music wire (# 12201, Century Spring Corp).

Stability model parameters for this spring were also determined as $\alpha = 2.639$, $\beta = 106.512$, $\gamma = 385$, $F_{max} = 3.3N$.

By substituting these values in Eq. 3.8 it becomes as follow:

$$F_s = 145.88\theta^4 - 40.36\theta^2 + 0.378\frac{\dot{\theta}}{\theta} + 3.3 \quad (3.9)$$

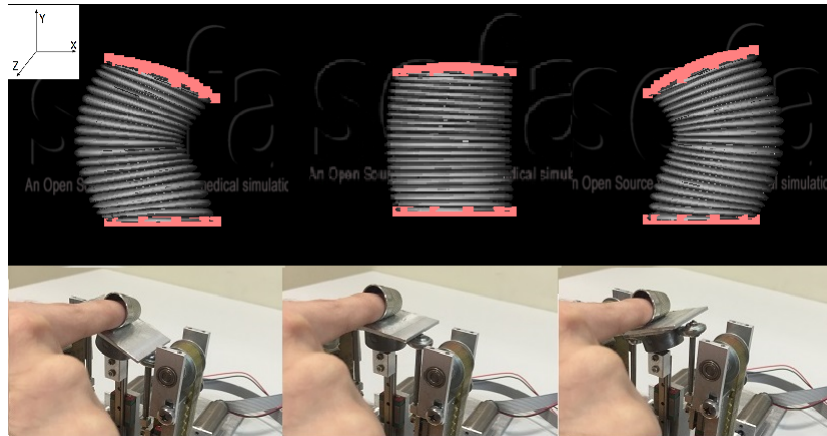


Figure 3.7 A virtual spring controlled by the haptic interface in translation (along Y axis) and rotation (around Z axis) degrees of freedom.

A critical problem arises here; since Cuevas et al. [5] performed a physical representation of the task they measured the angle cap and there was no need for calculation. However, since one of the input conditions to control the virtual spring in our application is isometric mode, we needed to find a relation between applied force and length of virtual spring to the angle of cap. A compression spring is loaded as a column and can buckle if it is too slender. Problem of buckling of springs is examined by their resistance to bending. Consider a spring of length L and coil radius $D/2$ subjected to bending moment M . It seems obvious that the effect is an angular rotation. By applying Castiglano's theorem we obtain the following expression:

$$\theta = M \int_0^{2\pi N a} \left(\frac{\sin^2 \alpha}{EI} + \frac{\cos^2 \alpha}{GJ} \right) \left(\frac{D}{2} d\alpha \right) \quad (3.10)$$

Here, $G = E/2(1 + \nu)$, and for a round wire, $J = 2I = \frac{\pi d^4}{32}$ which yields;

$$\theta = \frac{64MDN_a}{Ed^4} \left(1 + \frac{\nu}{2} \right) \quad (3.11)$$

Where:

M: Moment applied to spring cap

D: Spring diameter

N_a : Number of active coils (coils which are not compressed completely and can deform)

E: Modulus of elasticity

d: Wire diameter

According to Eq.3.11 rotational spring constant can be derived as:

$$K_{\theta} = \frac{64DN_a}{Ed^4} \left(1 + \frac{\nu}{2}\right) \quad (3.12)$$

Number of active coils were determined by subtracting solid length of spring from its free length divided by number of total coils the remaining, this way we were able to obtain the angle of the cap in isometric experiments. Stability criteria was when applied force to exerted endcap was less than or equal to the allowable force F_s . Graphical representation of the equation is illustrated in Figure 3.8. Therefore subjects should avoid inclining endcap. Provided that spring is compressed with zero angle, there is still a possibility buckling since maximum attainable compressive force is exceeded, hence it buckles.

3.2. Experimental Protocol

Fourteen subjects (8 male, 6 female) volunteered to participate in the study. Prior to the experiment they were asked to read the consent form and sign it. They were also given 30 Turkish Lira as an incentive to participate in the experiments. Majority of participants were right handed(12) and the other ones were left handed(2). Subjects were told that they had to control a virtual spring via multiple devices and with different sensory feedbacks. They had to compress a spring avoiding spring cap being tilted so that it would not buckle since we know that two critical factors in spring buckling are cap angle and applied force.

Seven experiments were designed to determine the contribution of position and force feedback on manipulation of the virtual spring. Each mode of these experiments are summarized in Table.3.2. Each mode consisted of two parts; training session and main session. Prior to each experiment, there was a briefing session for each subject to explain general objectives of the corresponding task and how to use each device. In

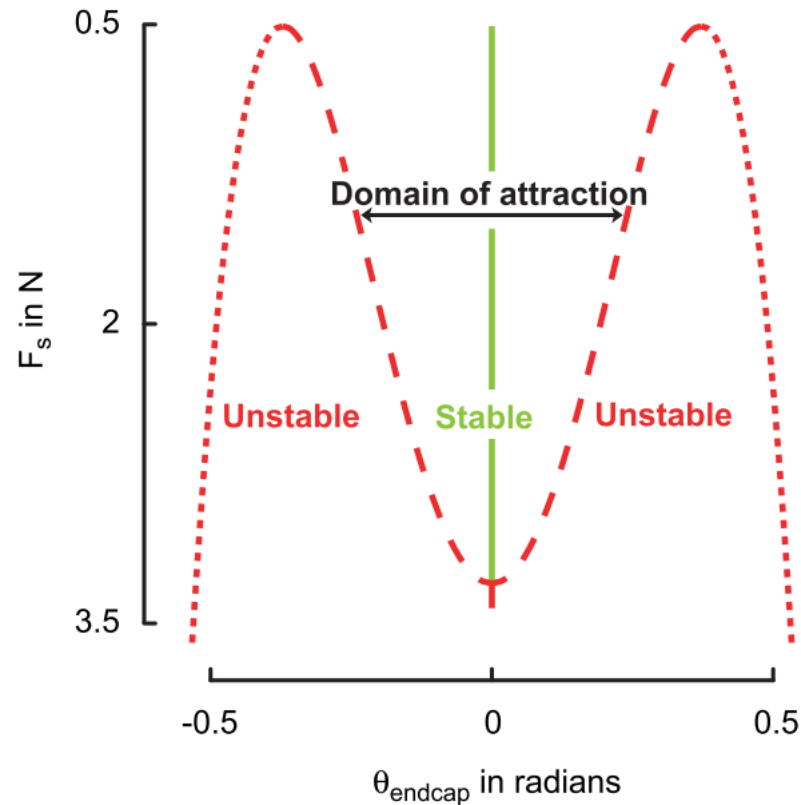


Figure 3.8 Graphical representation of buckling stability. As the angle is more deviated from zero value, allowable applying force is more limited hence increase probability of spring buckle [5].

the training session, subjects were allowed to interact with the corresponding device and they had to meet learning condition requirement. Learning condition was defined as three consecutive successful performance in each mode however, subjects were not aware of this matter. Main sessions consisted 10 trials of each mode. Participants were informed at the beginning and at the end of each training session and main session about the status they are in (whether they are in main session or training). At the end of each training session, subjects were asked to assign a number between one to five to each mode based on the difficulty of the task in that mode. Scoring principle was such that one represented “very easy” and five represented “very difficult”. Parameters which were recorded for both trial sessions and main sessions were whether the task was successfully completed or not, completion time in case of success and distance traveled as well as failure time in case of not completing the task.

They were asked to pay attention to their execution time and they were told that task completion time was recorded. However, they were advised not to move too quickly to avoid missing position registers. Additionally, subjects were asked to just look at the screen and try to pay attention to the light indicators as well. Before their first experience with any of the devices they were instructed about the general functionality and the feedback that they are going to receive to prepare them for the trial. It was assured that subjects realized that training session trials are as important as the main session ones.

In order to prevent any learning or habituation, we randomized task orders. Subjects were sitting on a chair comfortably while doing each task with their attention focused on the screen for receiving visual feedback. In each experiment there were light indicators (LED) which signaled participants to perform according to protocol. Primarily subjects began the task when green light was on and had to compress virtual spring until green light turned off; that was when red light was switched on. Red light stayed on for 5 seconds which indicated that subjects should keep the virtual spring at the same position. They were informed about completion of each trial by a yellow light. If they managed to complete the task without buckling, task was considered successful. In case of buckling, we recorded the position at which buckling occurred.

There were seven modes which contained different input and sensory substitution feedback. In the first three experiments subjects did not receive any sensory substitution feedback, these experiments were a baseline for us to analyze how well sensory substitution feedback could improve subjects' performance in the tasks with sensory substitution feedback. To decrease the break time between each mode of the experiment, corresponding codes for virtual reality and microcontrollers were prepared to be uploaded on each trial.

In the first mode (PFN) subjects were going to compress the virtual spring via haptic device with their dominant hand index finger while looking at the screen to get visual feedback. In this mode subjects were free to move the haptic device while a proportional spring force was exerted to their finger, hence they received position and

force feedback on the same hand.

In the second mode (PN) subjects interacted with the sensor device which did not deliver any kind of sensory substitution feedback. In this mode subject was able to move his finger freely without any force feedback. This kind of movement in which position feedback is available is termed as isotonic movement of muscles.

In the third mode of the experiment (FN), subjects pressed on the force sensor and had to control applied forces so that task would be completed without buckling of virtual spring. This kind of feedback in which muscles apply force but there is no resultant movement of muscles is called isometric movement.

In the fourth mode (PV) subjects repeated the same procedure as the one in the second experiment with an additional vibration feedback. Vibration feedback which maps the resultant force of the virtual spring was delivered to subjects on their contralateral hand. Both normal force and lateral force feedback were delivered on subject's forearm glabrous skin with 10 cm distance. The more subjects tilted or compressed the virtual spring the more noticeable vibration feedback was delivered to the subject as a representation of torque or normal force, respectively. In this mode contribution of wrong modality sensory substitution was assessed.

In the fifth experiment (FV), subjects applied force to the force sensor and position feedback was given to them in the form of vibration. Here sensory substitution feedback was received by subjects in a similar manner like the fourth experiment with the only difference that in this experiment vibration feedback was a representation of position and orientation, instead of force and torque.

In the sixth mode (PF) subjects were asked to place their dominant hand index finger in the thimble of the input device which guided the position of virtual environment while they should put their contralateral index finger on the haptic device. Here subjects were instructed to try to keep their finger stationary. The haptic device applied a force proportional to position of the virtual spring so subjects could receive

force feedback.

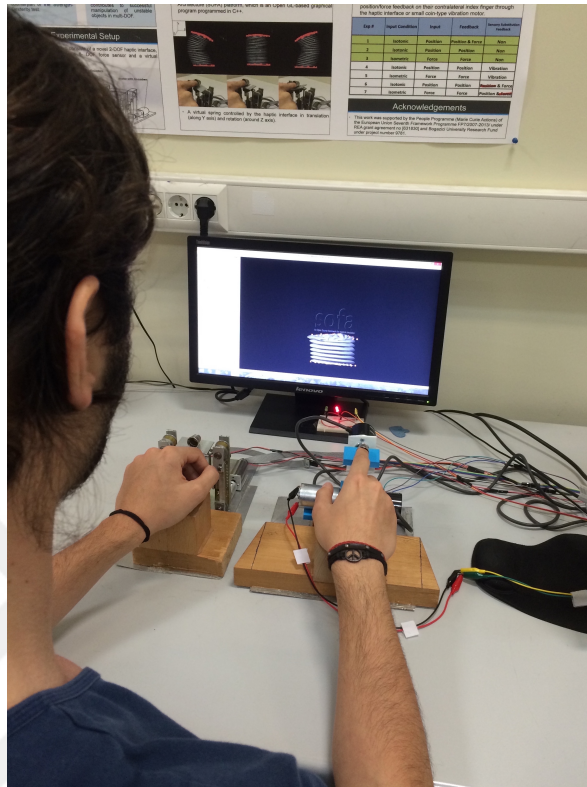


Figure 3.9 Psychophysical test. Subject is interacting with input device and is receiving force feedback on his contralateral hand index finger. Subject reached the goal position.

In the seventh mode (FP) subjects put their dominant hand index finger on the force sensor and tried to control the virtual spring via force input. Meanwhile subjects put their contralateral index finger in the haptic device from which they would receive position feedback of the virtual spring. This position feedback was proportional to displacement of virtual spring. Entire setup during an experiment is shown in Figure 3.9 and Figure 3.10.

In order to facilitate remembering each mode of the experiment in the following sections, we have devised an abbreviation for each mode. The first letter represents input type of that mode which is either P (Position) and F (Force). Second (and Third) letter indicates the input type P (Position), F (Force) and PF(Position and Force). Last letter represent type of sensory feedback which is N (No sensory feedback), V

(Vibration), F (Force) and P (Position). Obtained abbreviations and experimental procedure are explained in Table. 3.3.

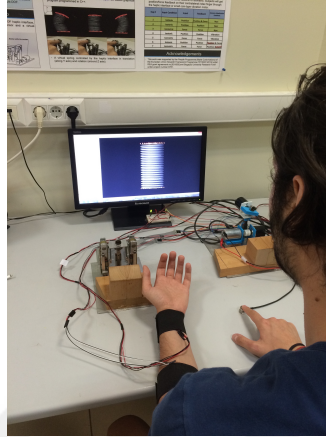


Figure 3.10 Psychophysical test. Subject is interacting with force sensor to compress the virtual spring.

Table 3.2 Different modes of psychophysical experiment. Modes; (1) Isotonic input with force feedback, (2) Isotonic input without force feedback, (3) Isometric input without position feedback, (4) Isotonic input with vibration feedback, (5) Isometric input with vibration feedback, (6) Isotonic input with sensory substitution of force, and (7) Isotonic input with sensory substitution of position.

Exp #	Input Condi- tion	Input	Feedback	Sensory sub- stitution feedback
1	Isotonic	Position & Force	Position	Non
2	Isotonic	Position	Position	Non
3	Isometric	Force	Force	Non
4	Isotonic	Position	Position	Vibration
5	Isometric	Force	Force	Vibration
6	Isotonic	Position	Position	Force
7	Isometric	Force	Force	Position

Table 3.3 Experimental procedure for different modes of the psychophysical test

Modes	Procedure
1 (PFN)	subject moves haptic device and feels position and force feedback on the same place without sensory substitution feedback
2 (PN)	subject moves sensor device and feels the position feedback without sensory substitution feedback
3 (FN)	subject applies force on force sensor and feels his applied force without sensory substitution feedback
4 (PV)	subject moves sensor device and receives vibration feedback on contralateral hand which maps virtual spring resistive force
5 (FV)	subject applies force on force sensor and receives vibration feedback on contralateral hand which maps position of virtual spring cap
6 (PF)	subject moves sensor device and receives the corresponding resistive force of virtual spring on his contralateral finger via haptic device
7 (FP)	subject applies force on the force sensor and receives corresponding position of virtual spring cap on his contralateral hand via sensor device

4. HAPTIC INTERFACE

In the following sections, first the design and development of our haptic interface are presented. On subsequent sections, physical and psychophysical evaluation of the setup are discussed.

4.1. Electro-mechanical Design

Designing an effective haptic interface which enables us to simulate such a complicated task demands a novel mechanisms. Technical drawings were developed in SOLIDWORKS software. The haptic interface is composed of a parallel mechanism, two DC motors with quadrature encoders (Maxon DCX22L and ENX 16 EASY) and a thimble (depicted in Figure 3.2, Right). Motors are powered by 12 V and their maximum power is 30mN at 1.33A, diameter of each motor is 22mm. Actuating haptic device is made of Aluminum by utilizing lathe.

Rotations of the motors are transmitted to translation and rotation of the thimble through a series of joints, belts, gears and linear rails . Figures 4.1 and 4.2 show our design and manufactured setup respectively. Linear rails allow each end of the plate move in one direction, so they constrain movement of plate in unwanted directions. Conversion of rotation to translation is accomplished via two gears connected to each other with a belt; by movement of any of the gears belt rolls on the gear, since plate ends are fixed on the belt by rotation of the gears plate ends are moved linearly. Couplings are responsible for transmitting motor power to the mechanism. Smooth rotation of gears is guaranteed by employing SKF needle bearings. All the main part are screwed to a plate in order to stabilize the setup. The encoders have a resolution of 1024 counts per turn which corresponds to translational resolution of 0.068 mm and rotational resolution of 0.16° . Motors are driven by two Pololu 18V7 motor controllers to give smooth and amplified signals to motors. This controller converts PWM signals to analog signals and also amplifies current corresponding to the input PWM signal. The latter seems critical in our application since each Arduino pin is capable of generating

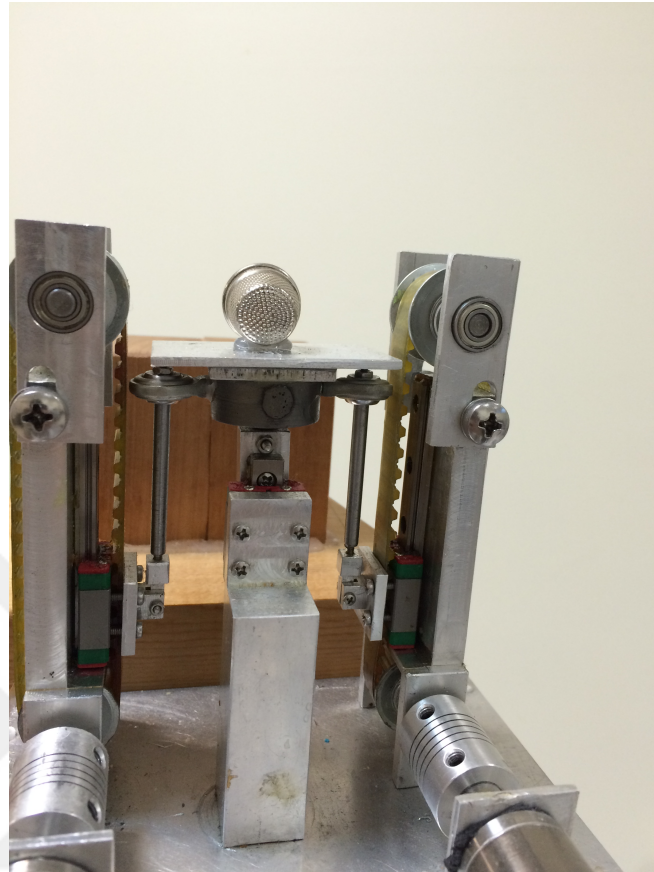


Figure 4.1 Designed mechanism of haptic device. Rotational movement of the motors are transformed to a combination of translation and rotation of the plate.

40 mA which is too low for the motors. Each controller is connected to an external power supply to provide necessary power for motors. Power supply output was limited to 12 V and 2 A to prevent any possible damage to motors.

4.2. Control Algorithms

Control algorithms are of paramount importance in haptic systems since their ultimate goal is to simulate an existing physical phenomenon. In this section control strategies to simulate real mechanical behavior of compression spring is described. In order to simulate a compression spring, we need to know their governing equations. To simulate spring behavior on the haptic device, we employed a proportional position controller on motors based on Hooke's law. In this manner, the moment system began reading encoder signals would be considered as the initial point of the system. Deviation from the initial point leads to an amount of error. After converting encoder

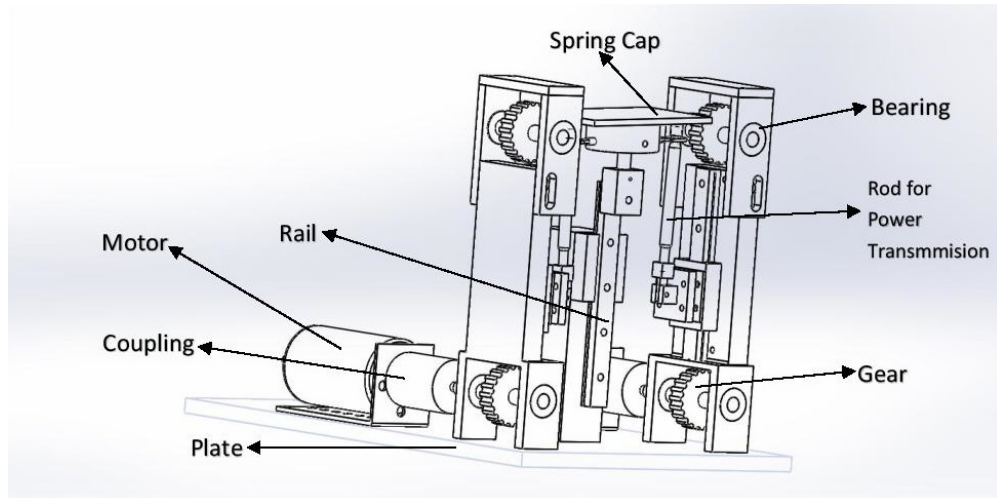


Figure 4.2 Technical design of haptic device including all the components.

position reading to millimeters, spring coefficient was multiplied by the error amount which is a direct exploitation of a spring model. Stiffness of the spring K_p , was 260 N/m . Assuming different forces are applied to two sides of spring cap the free body diagram is shown in Figure 4.3, there will be reaction forces resisting spring deformation; F_1 and F_2 which are the resulting linear components of spring constants and F_θ which is the torsional component of spring constant. Calculating the resulting moment about point O yields the following equation:

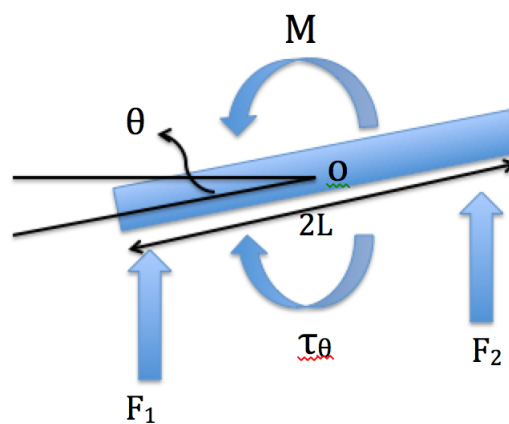


Figure 4.3 Spring cap free body diagram.

$$M = F_1L - F_2L + \tau_\theta \quad (4.1)$$

Furthermore, there is a relation between the applied moment and cap resistance to rotation.

$$\begin{aligned} M &= K_\theta\theta = 2F_\theta L + 2k\Delta xL \\ F_\theta &= \frac{K_\theta\theta - 2k\Delta xL}{2L} \\ F_\theta &= \frac{K_\theta\theta}{2L} - k\theta L \end{aligned} \quad (4.2)$$

The last expression yields the resulting torsional force due to rotation of spring endcap. K_θ is derived from Eq. 3.12. In this manner reaction forces due to compression of spring and rotation of the spring are decoupled which is how a real spring behaves.

Calculations regarding force output of the motors were carried out by multiplying position data by the spring constant of the simulated spring. Since commanding motors in an open-loop manner would not yield our desired result, a PD controller has been implemented. K_p and K_d coefficients were determined by trial and error which resulted in $K_p = 1.25$ and $K_d = 1$. Controller coefficients were selected in such a way that there would be a compromise between system stability and response time.

4.2.1. Admittance Control

Admittance controlled systems are based on the definition of a mechanical impedance, describing a transfer characteristics with force input and velocity output. These systems generate a position change with respect to a force input from the user. Here F is applied force by the operator which will be measured by the force sensor. An admittance coefficient is assigned to the virtual environment which will calculate resulting

displacement caused by the applied force. These joint angles will be a command for a PD position control of the haptic device. PD controller measures the position error between the current configuration of haptic device and virtual spring cap, calculated error and error difference, are multiplied to K_p and K_d coefficients respectively. General structure of control this strategy is illustrated in in Figure 4.4.

4.2.2. Impedance Control

Impedance controlled systems are based on the transfer characteristics of a mechanical impedance and are the structure of many kinaesthetic devices. They generate a force as output and measure a position as input as depicted in Figure 4.5. Here X is applied displacement by the user, which is applied to virtual environment as well. By assigning a stiffness coefficient to virtual environment we can gain the corresponding reflected force of the haptic device.

A separate control method utilized to transfer position or force data from SOFA to Arduino; in this approach since data was sent consecutively, a method was needed to distinguish each individual data. To achieve this goal we placed each portion of data between some delimiters. A delimiter is a sequence of one or more characters used to specify the boundary between separate, independent regions. “/P” represented the delimiter for position data or normal force and “/R” indicated the rotation of cap or moment applied to the cap. By extracting position and rotation data from data stream and by having previous configuration of haptic device an error was generated which determined PWM applied on each motor. Mathematical representation of our device kinematics can be demonstrated as:

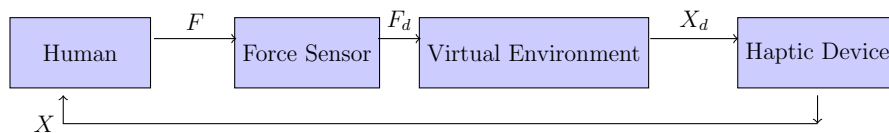


Figure 4.4 Admittance control block diagram.

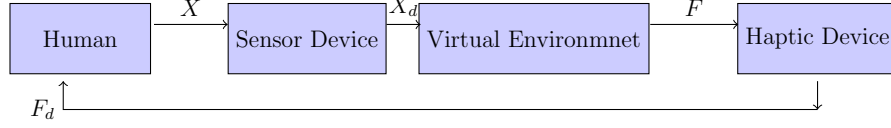


Figure 4.5 Impedance control block diagram.

$$\begin{aligned}
 LM &= Pos + Rot \\
 RM &= Pos - Rot
 \end{aligned}
 \tag{4.3}$$

Where:

$LM = LeftMotorPosition$

$RM = RightMotorPositions$

$Pos = PositionofCap$

$Rot = AngleofCap$

4.3. Evaluation

4.3.1. Physical Evaluation

There is general consensus about haptic device validation and identification parameters [125]. Since our setup operates both in static range and dynamic range, all the physical evaluation tests seem necessary. Therefore, we implemented the common evaluation practices available in the literature to validate our setup [125].

4.3.1.1. Friction Compensation. For friction and gravity compensation, we measured the resistive forces while moving the end effector manually across the workspace of the haptic device with a constant speed. A force sensor (ATI Nano 17) was used for the measurement as shown in Figure 4.6 (orange curve), the reaction forces in upward movement and downward movement converge to a certain amount, except for the distal areas of the rail. We assumed that friction force was constant across the rail

when moving in one direction. Hence we allocated a constant amount of force for

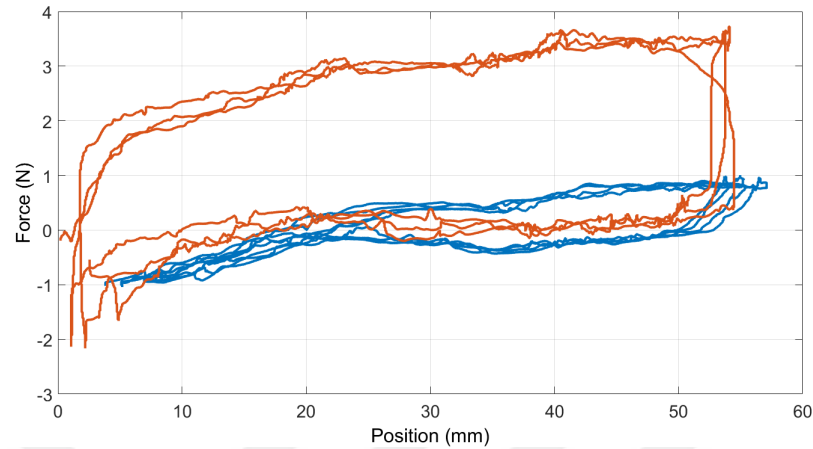


Figure 4.6 Resistive forces without compensation (Orange) and with friction compensation (Blue).

compensation of gravity and friction force based on the direction of movement. The motors are driven with a certain input to apply these direction-dependent compensation forces to the haptic interface. After the gravity and friction compensation, the reaction forces were measured again. The results are presented as blue lines in Figure 4.6. As seen in the figure, the resisting force is considerably less when gravity and friction compensation is applied. In this case the resisting force does not exceed 1 N throughout the workspace.

4.3.1.2. Static Response. In order to calibrate forces applied to the end effector by the motors, motor driver input from Arduino was recorded and the corresponding force generated by the motors were measured. Thus relation between motor commands and actual generated forces were obtained as shown in Eq. 4.4.

$$\tau_m = 204.6F + 133 \quad (4.4)$$

where;

τ_m : Motor Output Torque

4.3.1.3. Input-Output Curve. One of the primary specifications of a haptic device is maximum force output capability. In order to measure force output capability of the haptic device the force sensor (ATI Nano 17) shown in Figure 3.3 was attached between the tip of the device and a stationary rigid constraint. Output forces were measured while the motors were commanded with a slowly increasing and decreasing ramp input. Motors were driven up to their specified nominal torque. We also obtained the nominal force of motors when supplied with sufficient amount of current by utilizing motor data sheet which maps resultant motor force to current supplied to the motor. As motors were fixed and did not rotate, corresponding currents represent the stall torques and we can be sure that motors apply the amount of force indicated in the data sheet. We loaded and unloaded motors in two conditions:

- a) Without compensating for the device self weight and friction of the rails.
- b) With implementation of friction compensation strategy.

Results showed that there was a noticeable hysteresis between loading and unloading which was due to existence of friction in the rail however the hysteresis decreases obviously when friction compensation was added to the actuation loop, which can be seen in Figure 4.7. It is also worth to mention that non linearity of the system decreases as friction is compensated however, hysteresis of the setup still is a noticeable value.

To validate whether our setup is able to render virtual springs in a transparent manner, we simulated a series of springs with certain stiffness and measured the output force while the virtual spring was pressed via the haptic device. As an example spring force versus position is plotted for a virtual spring having a stiffness of $K=760$ N/m (Figure 4.8).

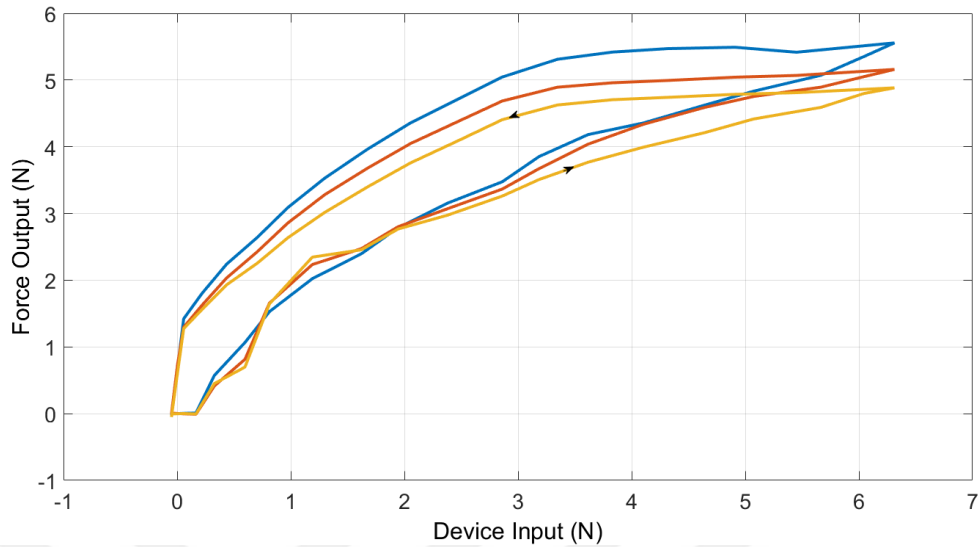


Figure 4.7 Device input versus force output with friction compensation.

Five different springs were simulated. Their stiffness values and the measured values are tabulated in Table 4.1. This procedure was repeated 5 times for each spring.

Data presented in Table 4.1 shows that the rendered stiffnesses closely match the

Table 4.1 Intended and measured spring stiffness

Spring Constant (N/m)	Spring 1	Spring 2	Spring 3	Spring 4	Spring 5
Intended	260	760	1280	2100	3000
Measured	256 ± 10.13	768 ± 10.13	1208 ± 47.19	2014 ± 47.74	2940 ± 103.1

intended values. Hence we can claim that our haptic device can be regarded as a reliable instance of a spring rendering system.

4.3.2. Psychophysical Evaluation

Although the physical evaluation presented previously showed that the haptic interface was able to render springs sufficiently, we conducted a psychophysical test to evaluate the perceptual characteristics of the setup. In this test participants were asked to distinguish the difference between real and virtual springs. The purpose of this study was to evaluate how precise subjects can distinguish stiffness between virtual and real springs and determine baseline parameters for further application of our setup.

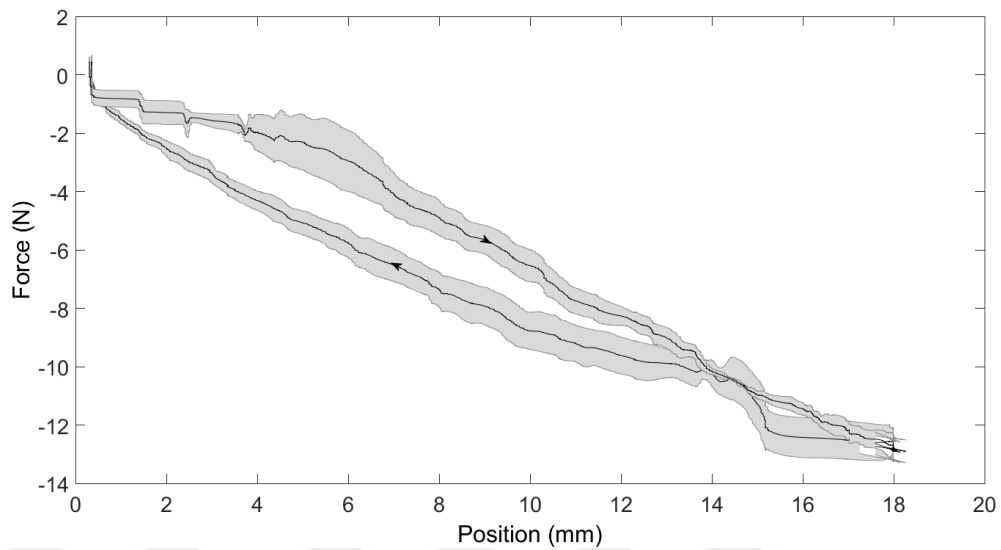


Figure 4.8 Virtual spring simulation. Solid line and shaded area represent the mean and the standard deviation of the five measurements, respectively. Arrow indicates the direction of movement

4.3.2.1. Subjects. Seven volunteers (2 women and 5 men) aged between 22 and 28 participated in the experiment. One subject was left-handed and six were right-handed. All subjects were able-bodied persons who did not suffer from any motor skill difficulty. None of the subjects was familiar with any kind of haptic interface.

4.3.2.2. Procedure. Each subject was briefed about the experimental procedure and trained how to interact with the system. Ethical consent was taken from each volunteer before the beginning of the experiment. Before we start the experiment, subjects were given five samples of real springs to work with so that they could gain an insight about stiffness range of the springs used in the experiment. Our experimental design consisted of two tasks; pushing real springs through the input device and virtual springs through the haptic interface. Subjects were looking at the virtual spring model on the screen on both cases. Subjects' vision was occluded by covering the entire setup with a piece of fabric so they did not see which device they are interacting with. Thus, they did not have any visual cue about whether they were touching a real or a virtual spring. They had to bring their dominant hand under the fabric and experimenter guided their index finger inside the thimble which was mounted on the end effector as

shown in Figure 4.9. Subjects were instructed not to start the trial until experimenter gave them permission to do so. Subjects were asked to compare two springs and state verbally whether they felt different or not. If subjects indicated that the springs felt different, they were asked to choose the stiffer spring by saying “left” or “right”. Their answers were recorded in the experiment form. Subjects were allowed to retry each spring as many times as they wished. Five different springs were used in the experiment. Their stiffnesses were at least 22% different from each other in order to have perceptually different springs[53]. Each real spring was compared with the virtual implementation of the other four springs. The whole experiment was repeated 3 times for each subject which lead to a total number of 60 trials. Virtual and real spring combination sequence was randomized using a MATLAB code so subjects would not become biased or learn the sequence of incoming trials. Overall the experiment lasted approximately 45 minutes for one subject. A two-minute-break was given to subjects in the middle of the experiment in order to prevent finger fatigue.

4.3.2.3. Results. Responses obtained from subjects were analyzed in terms of correct discrimination of spring stiffness. Results are presented in Table 4.2. As we had chosen the springs in a way to have stiffness differences higher than the just-noticeable-difference of stiffness

Table 4.2 **Experimental Setup Results**

Experimental Results								
	Sub1	Sub2	Sub3	Sub4	Sub5	Sub6	Sub7	Average(%)
Correct Answers (%)	44(73)	40(67)	44(73)	42(70)	50(83)	42(70)	44(73)	72.9

which is conservatively 22% [15], we would expect 100% correct answer for fully-transparent haptic rendering.

An average of 72.9% which is well above the level of chance, indicates that the virtual springs rendered by the haptic device closely follow the intended spring behavior.

The experimental results showed that the subjects were able to correctly discriminate springs even if they were virtual which demonstrates effectiveness of our setup. Intrinsic perceptual differences between the haptic device and the input device made subjects consider the haptic device to be stiffer than the other one. Another reason which lead to this perception is the fact that because of active feedback, such as friction compensation in the haptic interface and some ripples in its movement, subjects mistakenly interpreted the virtual spring stiffer (they misinterpret mechanical actuation as stiffer). This drawback is inevitable in haptic devices due to mechanical and electrical characteristics of a mechatronic system. Usage of higher precision components might diminish this obstacle. Another reason which made the virtual spring be felt stiffer is the asymmetries in the rails and overconstraints in the system. These overconstraints were unavoidable in designing the parallel kinematic structure of the mechanism.

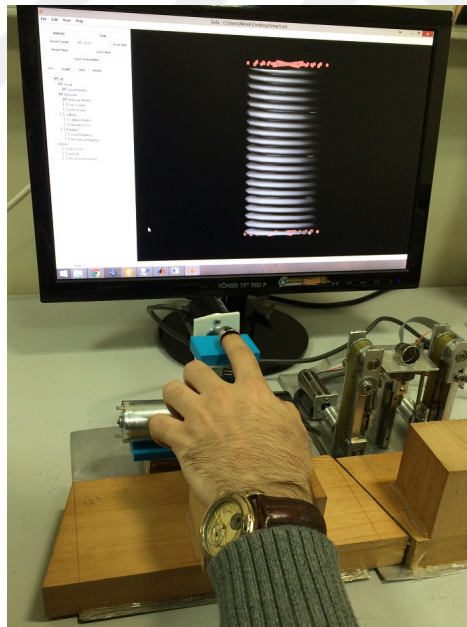


Figure 4.9 The input device (left) has isotonic input capability and the haptic interface (right) is an impedance-type device .

5. RESULTS AND DISCUSSIONS

5.1. Results of Psychophysical Study

Analysis of subjects' performance in the training session can provide us with information about subjects' learning process. In this regard, the first feature of the experiment which seems significant is the number of trials before accomplishing three consecutive successful task completion. It is shown in Figure 5.1 that subjects performed better mainly in tasks in which they receive position feedback. Number of trials in training based on modes are significantly different ($p=0.002$).

Success rate can be considered as the first performance metric in our psychophysical test since it represents compression of virtual spring without buckling. Figure 5.2 shows the mean success rates for each mode in the main session. Statistical analysis was performed on the experimental data with SPSS. One-way ANOVA analysis showed a significant difference between the success rates ($p = 0.005$). We performed a Tukey HSD Post-Hoc analysis for further investigation. It was observed that there were significant differences between PN (i.e., isotonic input without force feedback) and FN (i.e., isometric input without position feedback) as well as between PN and PF

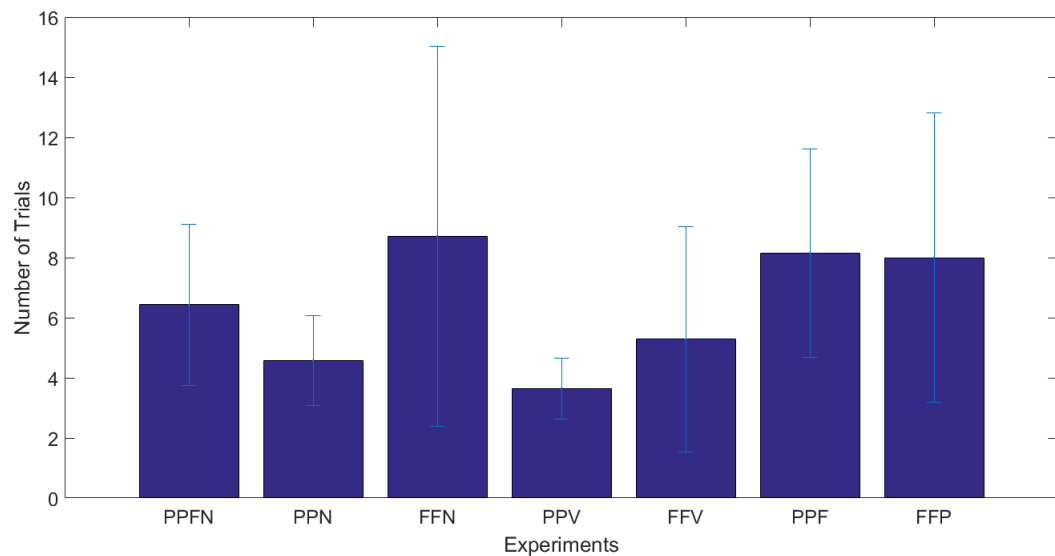


Figure 5.1 Mean values of number of trials before achieving the learning condition .

Table 5.1 ANOVA results and Post Hoc analysis for number of trials in training

Factors	df	F	Sum of Squares	Significance	Mean of Squares
No. Trials Training	F(6,91)	3,793	323.98	p=0.002	53.997
Tukey HSD Post Hoc					
Mode 1	Mode 2	Mean Difference		Significance	
FN	PV	5.071		p=0.01	
PF	PV	4.5		p=0.034	
FP	PV	4.357		p=0.045	

(i.e., isotonic input with sensory substitution of force) modes ($p = 0.04$ and $p = 0.026$, respectively). It can be seen that the highest rate of success belongs to the PN mode (87%) and the lowest performance was recorded in the PF mode (71%).

Another analysis which was conducted on the success rates was a two-way ANOVA. By eliminating PFN mode, we categorized the independent variables based on input type (two levels; isotonic and isometric) and the type of sensory substitution (no, modality-mismatched and modality-matched sensory feedback). Results detected a significant difference between the modality-matched and the modality-mismatched cases as well as between no feedback and modality-matched feedback with respective p -values of $p = 0.004$ and $p = 0.031$. Relation between modalities and input modes with respect to success rate are shown in Figure 5.3. No significant difference was observed between

Table 5.2 ANOVA results and Post Hoc analysis for success rate in main session

Factors	df	F	Sum of Squares	Significance	Mean of Squares
Success Rate Main Session	F(6,980)	3.134	3.224	p=0.005	0.537
Tukey HSD Post Hoc					
Mode1	Mode2	Mean Difference		Significance	
PN	FN	0.15		p=0.04	
PN	PF	0.1571		p=0.026	

different types of input mode.

Another approach in evaluation of subjects' performance is to assess their results based on the deviation from the goal position in the failed trials. Since this task

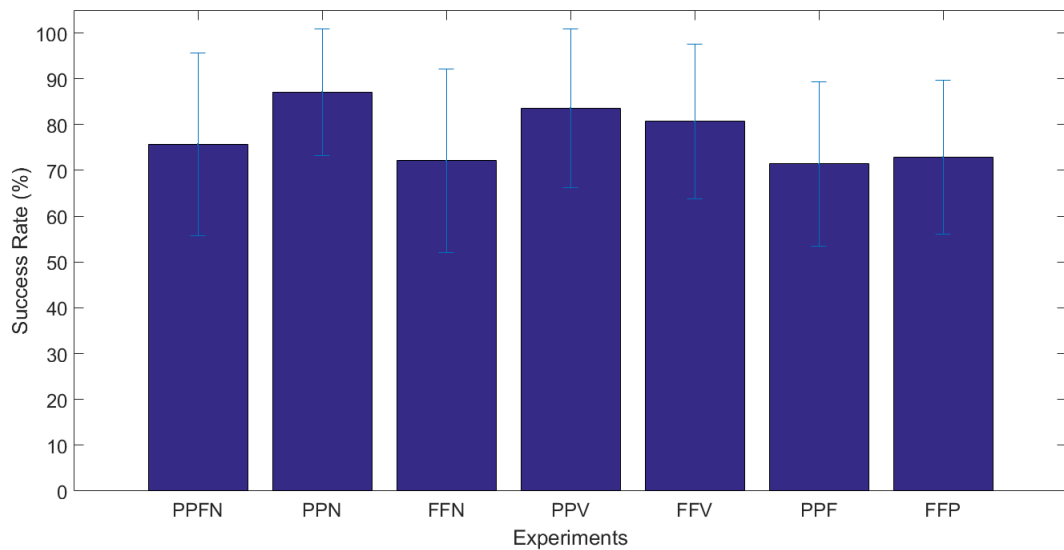


Figure 5.2 Success rates for each mode of the experiments.

Table 5.3 Results of two-way ANOVA.

Factors	df	F	Sum of Squares	Significance	Mean of Squares
Feedback Type	F(2,834)	4.483	1.517	p=0.012	0.758
Post Hoc					
Feedback Type 1	Feedback Type 2	Mean Difference		Significance	
Mismatched	Matched	0.1		p=0.004	
No	Matched	0.075		p=0.031	

is a complicated targeting task considering distance error seems a logical approach. A one-way ANOVA analysis was conducted on the mean positioning error shown in Figure 5.4. ANOVA analysis resulted in a significant difference. It seems apparent that participants deviated much more in isotonic mode. Mentioned ANOVA statistical values are summarized in Table. 5.5.

5.2. Discussion

By taking a look at data from trial numbers in training we can claim that it fortifies our hypothesis which considers the increase in complexity of the task by adding

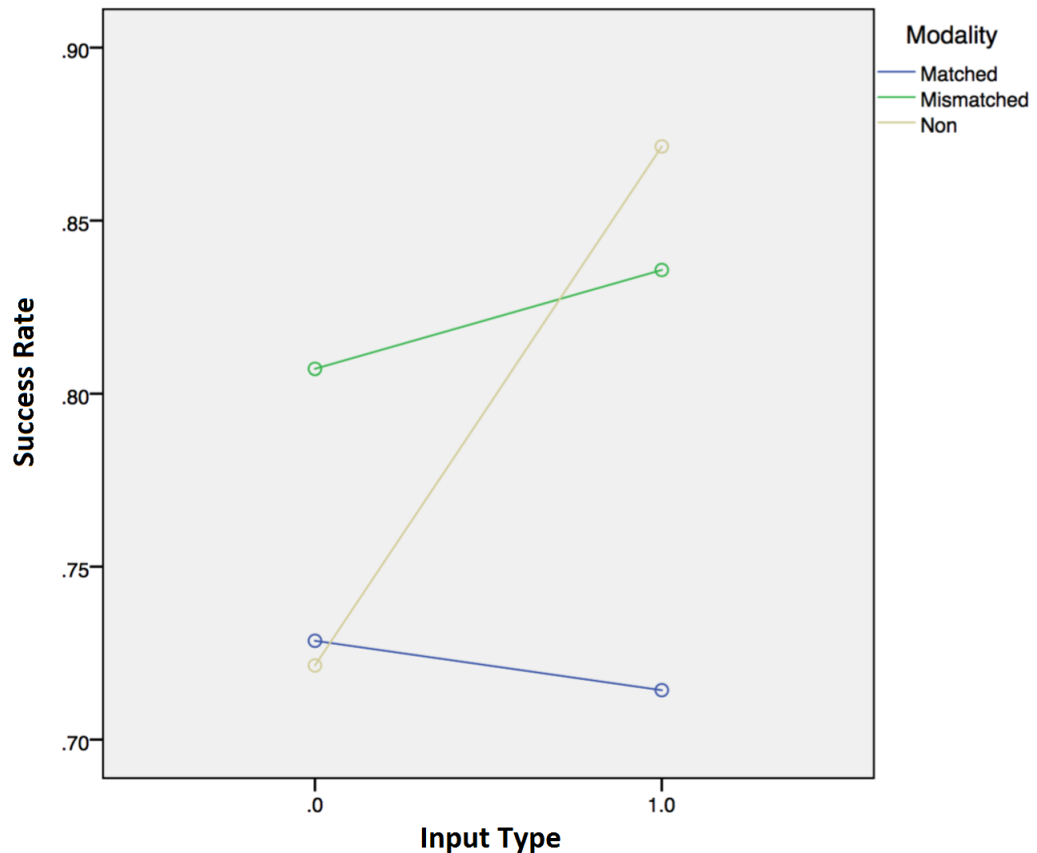


Figure 5.3 Participants' success rate based on input mode and sensory substitution method.

sensory information to the task. Unlike main session in which PN mode resulted in the best performance, the best results in training were obtained in PV mode. Hence, we can claim that subjects learnt faster when sensory substitution feedback was more intuitive and interpretable.

Having obtained the mentioned results, we hypothesize that sensory feedback not only gave subjects extra information about the status of virtual spring it also made them more cautious about their performance. Another issue which should be considered is intuition and convenience of feedback for sensory system and interpretability of delivered feedback. Keeping these aspects in mind, the obtained results make sense since subjects regarded the experiment as a simple positioning task in PN mode and did not pay attention to other features of the simulated system. This can be justified by looking at the completion time of PN mode shown in Figure 5.5. Similarly the results of the experiment in PF mode can be justified in terms of intuition and amount

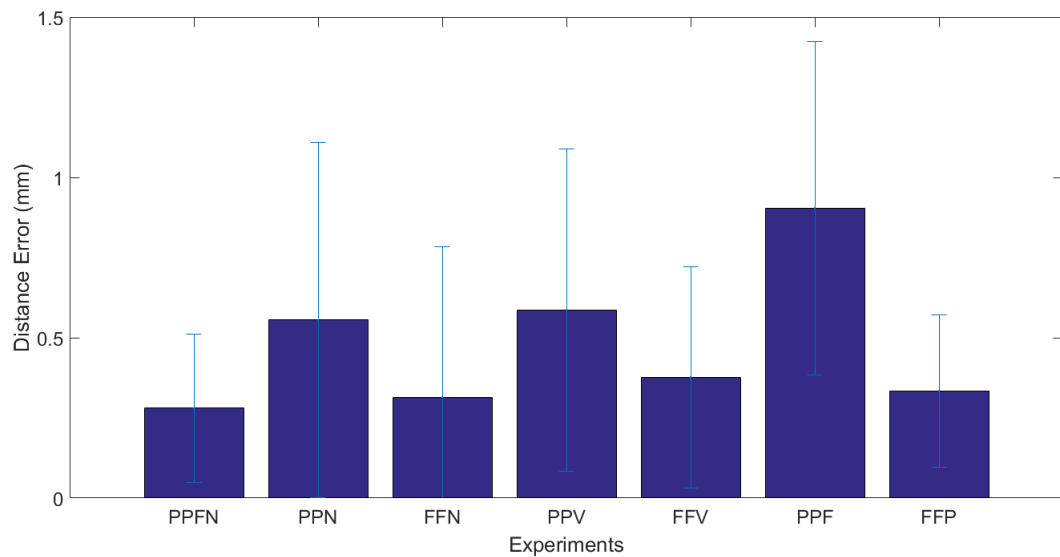


Figure 5.4 Mean value of error distance. Horizontal axes are the modes of experiment, vertical axes are the corresponding error distance values.

of information provided to the subject. Another issue in PF mode, which should not be ignored, is the extra cognitive load applied to subjects. Since we asked them to keep their contralateral finger stationary, this required simultaneous attention to task performance and applied reactive force on the haptic device. This can be justified by looking at subjects' completion time in Figure 5.5. From biological perspective it can be argued that since in the sixth and seventh modes cognitive activation of both hemispheres of the brain are required this makes the task more demanding compared to trials in which one hemisphere is engaged in task execution.

Regarding deviation error, we reckon resulted distinguishable difference can be caused by lack of sensory information or subjects' insufficient attention to additional force feedback since they considered it a distraction, enforced cognitive load (especially in PF mode) can be mentioned as another contributor.

Enforced cognitive load is reinforced by the obtained results from the survey acquired from subjects. As it is evident from Figure 5.6 PF mode was rated the most difficult mode. PFN mode accompanies PF, subjects acquired higher success rate in PFN mode since both position and force information were delivered to the same region of the limb

Table 5.4 ANOVA results and Post Hoc analysis for distance error

Factors	df	F	Sum of Squares	Significance	Mean of Squares
Feedback Type	F(6,218)	6.258	51.558	p=0	8.593
Tukey HSD Post Hoc					
Mode 1	Mode 2	Mean Difference		Significance	
PF	PFN	1.356		p=0	
PF	FN	1.198		p=0	
PF	FV	1.131		p=0.003	
PF	FP	1.343		p=0	

Table 5.5 ANOVA results.

Factors		Sum of Squares	Significance	Mean Squares
No. of Trials Training	F(6,91)	323.98	p=0.002	53.997
Success Rate Main Session	F(6,973)	3.224	p=0.005	0.537
Distance error main session	F(6,212)	51.558	p=0	8.593
Modality	F(2,840)	1.516	p=0.012	0.758

(collocated sensory feedback) which made interpretation of sensory information more intuitive.

We reckon that these reasons contributed to subjects' performances significantly. Another issue to mention is the importance of subjects engagement in a task which is able to attract them; drawing subjects' full attention to the task is an important feature of such psychophysical experiments. Subjects claimed that they were captivated by the developed system and for majority of them this experiment appeared as a game which can be regarded as an advantage of our setup.

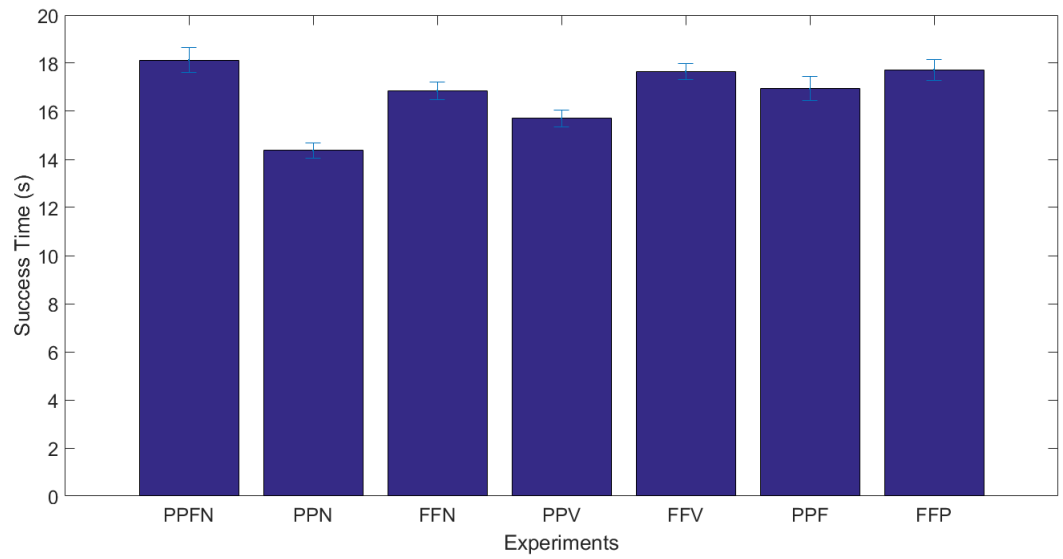


Figure 5.5 Elapsed Time for Successful Trials in Main Session.

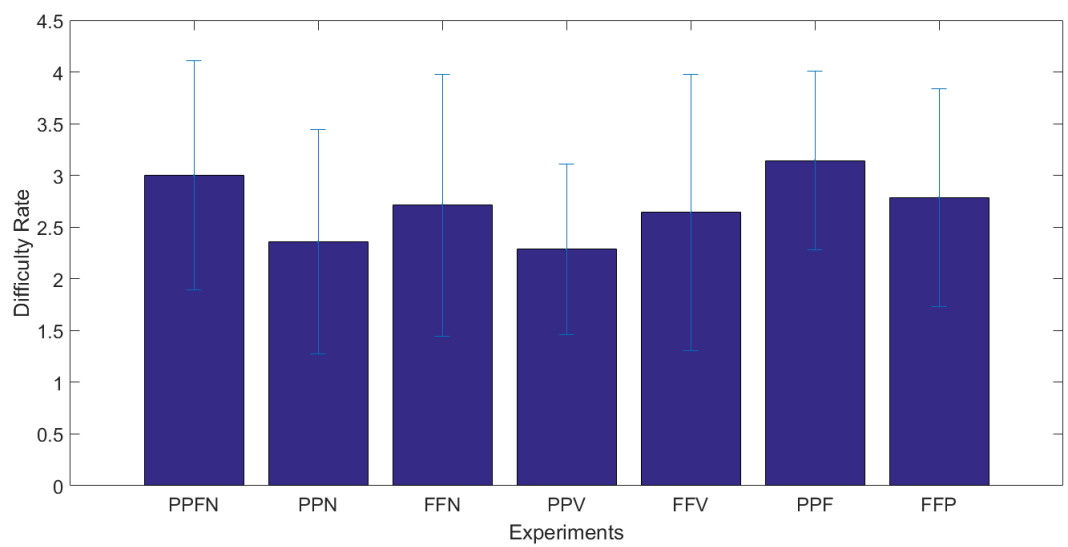


Figure 5.6 Mean value of subjects' difficulty rating .

6. CONCLUSION

A new method was developed to evaluate contribution of sensory substitution of force and position feedback on performance of a multi-DOF dynamic task. According to the attained results, we can claim that sensory substitution does not affect manipulation of an object which necessitates coordination of finger position and force. However, providing force related information, either directly or via sensory substitution feedback, reduced deviation from goal position in case of failure which can be an indication of increased precision which is expected since “Strength-Dexterity” is based on coordination of forces as well as positions. Finally we can add that delivering an easily interpretable feedback which consider the concept of sensory collocation can play an important role in successful completion of such exercises. By obtaining the results from these experiments we were able to determine how much and in what manner sensory substitution contributes to successful completion of a dynamic task and whether it has a constructive effect on subjects’ performance or not.

6.1. Contributions

A great amount of effort is directed towards enhancement of state-of-the-art upper-limb robotic prostheses, however they have not been adequate enough to yield desirable empirical results in application. It seems that devising a psychophysical design which enforces reliance of participants on haptic feedback rather than vision is an important issue to be considered. A part of this inadequacy can be contributed to the simplicity of designed task which in most cases were targeting position [15]. In a majority of conducted studies position information solely sufficed to accomplish the task. In this study, we investigated the effect of individual sensory substitution modalities in 2-DOF in performing a dynamic task on able-bodied subjects. This setup is novel in many terms such as: nature of the task, higher freedom which elevated task difficulty, impedance and admittance control possibilities and a novel haptic device.

6.2. Future Works

Some flaws existed in the design and control of the experimental setup which can be alleviated in future studies. There was a sampling frequency limitation enforced on our system due to processing incompetency of Arduino. Currently available real-time equipment such as National Instrument data acquisition card and motor control modules can remove these constraints and elevated system response. Another intrinsic complication lay in sensory feedback method we utilized in PF mode of our experiments which caused inequality of conditions in terms of cognitive processing requirements and sensory processing ability. By applying further enhancements to current setup psychophysical scenarios can be devised which does not require any consideration from subject's side. We believe this surely enhances subjects' performance and dismisses faults stemmed from participant's inaccuracies which makes obtained results more objective. The last proposal to improve operation of the current system is to develop a new method in which a collocated sensory feedback is delivered to subjects since this adds to intuitiveness of the haptic feedback which is an ultimate goal in design of any haptic system. This study can be a bedrock and a guide for the researchers who want to invent a haptic device in hope of delivering transparent sensory information to the users of prostheses.

REFERENCES

1. Ziegler-Graham, K., E. J. MacKenzie, P. L. Ephraim, T. G. Trivison and R. Brookmeyer, “Estimating the Prevalence of Limb Loss in the United States: 2005 to 2050”, *Archives of Physical Medicine and Rehabilitation*, Vol. 89, No. 3, pp. 422–429, 2008.
2. Dudkiewicz, I., R. Gabrielov, I. Seiv-Ner, G. Zelig and M. Heim, “Evaluation of prosthetic usage in upper limb amputees.”, *Disability and rehabilitation*, Vol. 26, No. 1, pp. 60–63, 2004.
3. Schultz, A. E., S. P. Baade and T. a. Kuiken, “Expert opinions on success factors for upper-limb prostheses.”, *Journal of rehabilitation research and development*, Vol. 44, No. 4, pp. 483–489, 2007.
4. Kuschel, M., M. Di Luca, M. Buss and R. L. Klatzky, “Combination and integration in the perception of visual-haptic compliance information”, *IEEE Transactions on Haptics*, Vol. 3, No. 4, pp. 234–244, 2010.
5. Venkadesan, M., J. Guckenheimer and F. J. Valero-Cuevas, “Manipulating the edge of instability”, *Journal of Biomechanics*, Vol. 40, No. 8, pp. 1653–1661, 2007.
6. D’Alonzo, M. and C. Cipriani, “Vibrotactile sensory substitution elicits feeling of ownership of an alien hand.”, *PloS one*, Vol. 7, No. 11, p. e50756, 2012.
7. Østlie, K., I. M. Lesjø, R. J. Franklin, B. Garfelt, O. H. Skjeldal and P. Magnus, “Prosthesis rejection in acquired major upper-limb amputees: a population-based survey”, *Disability and Rehabilitation: Assistive Technology*, Vol. 7, No. 4, pp. 294–303, 2012.
8. Sainburg, R. L., M. F. Ghilardi, H. Poizner and C. Ghez, “Control of limb dynamics in normal subjects and patients without proprioception.”, *Journal of neurophysiology*, Vol. 73, No. 2, pp. 820–835, 1995.
9. Wolpert, D. M., R. Miall and M. Kawato, “Internal models in the cerebellum”, *Trends in Cognitive Sciences*, Vol. 2, No. 9, pp. 338–347, sep 1998.

10. Valero-Cuevas, F. J., F. E. Zajac and C. G. Burgar, “Large index-fingertip forces are produced by subject-independent patterns of muscle excitation”, *Journal of Biomechanics*, Vol. 31, No. 8, pp. 693–703, 1998.
11. Valero-Cuevas, F. J., “Predictive modulation of muscle coordination pattern magnitude scales fingertip force magnitude over the voluntary range.”, *Journal of neurophysiology*, Vol. 83, No. 3, pp. 1469–1479, 2000.
12. Valero-Cuevas, F. J., N. Smaby, M. Venkadesan, M. Peterson and T. Wright, “The strength-dexterity test as a measure of dynamic pinch performance”, *Journal of Biomechanics*, Vol. 36, pp. 265–270, 2003.
13. Valero-Cuevas, F. J., “An integrative approach to the biomechanical function and neuromuscular control of the fingers”, *Journal of Biomechanics*, Vol. 38, No. 4, pp. 673–684, 2005.
14. Gurari, N., K. J. Kuchenbecker and A. M. Okamura, “Stiffness discrimination with visual and proprioceptive cues”, *Proceedings - 3rd Joint EuroHaptics Conference and Symposium on Haptic Interfaces for Virtual Environment and Teleoperator Systems, World Haptics 2009*, pp. 121–126, 2009.
15. Blank, A., A. M. Okamura and K. J. Kuchenbecker, “Identifying the role of proprioception in upper-limb prosthesis control”, *ACM Transactions on Applied Perception*, Vol. 7, No. 3, pp. 1–23, 2010.
16. Stepp, C. E. and Y. Matsuoka, “Vibrotactile sensory substitution for object manipulation: amplitude versus pulse train frequency modulation”, *Neural Systems and Rehabilitation Engineering, IEEE Transactions on*, Vol. 20, No. 1, pp. 31–37, 2012.
17. Antfolk, C., M. D’Alonzo, B. Rosén, G. Lundborg, F. Sebelius and C. Cipriani, “Sensory feedback in upper limb prosthetics.”, *Expert review of medical devices*, Vol. 10, No. 1, pp. 45–54, 2013.
18. Atkins, D. J., D. C. Heard and W. H. Donovan, “Epidemiologic Overview of Individuals with Upper-Limb Loss and Their Reported Research Priorities”, *JPO Journal of Prosthetics and Orthotics*, Vol. 8, No. 1, pp. 2–11, 1996.

19. Cordella, F., A. L. Ciancio, R. Sacchetti, A. Davalli, A. G. Cutti, E. Guglielmelli and L. Zollo, "Literature review on needs of upper limb prosthesis users", *Frontiers in neuroscience*, Vol. 10, 2016.
20. Wright, T. W., A. D. Hagen and M. B. Wood, "Prosthetic usage in major upper extremity amputations.", *The Journal of hand surgery*, Vol. 20, No. 4, pp. 619–22, jul 1995.
21. Heger, H., S. Millstein and G. a. Hunter, "Electrically powered prostheses for the adult with an upper limb amputation.", *The Journal of bone and joint surgery. British volume*, Vol. 67, No. 2, pp. 278–281, 1985.
22. Dohn, P., X00E, Lek, P. Gajdo, X and T. Peterek, "Human activity recognition on raw sensor data via sparse approximation", *Telecommunications and Signal Processing (TSP), 2013 36th International Conference on*, pp. 700–703, 2013.
23. Gonzalez, D. S. and C. Castellini, "A realistic implementation of ultrasound imaging as a human-machine interface for upper-limb amputees", *Frontiers in Neuro-robotics*, Vol. 7, No. OCT, 2013.
24. Wininger, M., N.-H. Kim and W. Craelius, "Pressure signature of forearm as predictor of grip force.", *Journal of rehabilitation research and development*, Vol. 45, No. 6, pp. 883–892, 2008.
25. Pasquina, P. F., M. Evangelista, A. J. Carvalho, J. Lockhart, S. Griffin, G. Nanos, P. McKay, M. Hansen, D. Ipsen, J. Vandersea, J. Butkus, M. Miller, I. Murphy and D. Hankin, "First-in-man demonstration of a fully implanted myoelectric sensors system to control an advanced electromechanical prosthetic hand.", *Journal of neuroscience methods*, Vol. 244, pp. 85–93, 2015.
26. Dhillon, G. S., S. M. Lawrence, D. T. Hutchinson and K. W. Horch, "Residual function in peripheral nerve stumps of amputees: Implications for neural control of artificial limbs", *Journal of Hand Surgery*, Vol. 29, No. 4, pp. 605–615, 2004.
27. Hebert, J. S., K. Elzinga, K. M. Chan, J. Olson and M. Morhart, "Updates in Targeted Sensory Reinnervation for Upper Limb Amputation", *Current Surgery Reports*, Vol. 2, No. 45, pp. 1–9, 2014.

28. Kung, T. a., R. a. Bueno, G. K. Alkhalefah, N. B. Langhals, M. G. Urbanchek and P. S. Cederna, “Innovations in prosthetic interfaces for the upper extremity.”, *Plastic and reconstructive surgery*, Vol. 132, No. 6, pp. 1515–1523, 2013.
29. Dhillon, G. S. and K. W. Horch, “Direct neural sensory feedback and control of a prosthetic arm”, *IEEE Transactions on Neural Systems and Rehabilitation Engineering*, Vol. 13, No. 4, pp. 468–472, 2005.
30. Carey, S. L., D. J. Lura and M. J. Highsmith, “Differences in myoelectric and body-powered upper-limb prostheses: Systematic literature review”, *Journal of Research Rehabilitation and Development*, Vol. 52, No. 3, pp. 17–19, 2014.
31. Kuchenbecker, K. J., N. Gurari and A. M. Okamura, “Effects of visual and proprioceptive motion feedback on human control of targeted movement”, *2007 IEEE 10th International Conference on Rehabilitation Robotics, ICORR’07*, pp. 513–524, 2007.
32. Kaczmarek, K. a., J. G. Webster, P. Bach-y Rita and W. J. Tompkins, “Electrotactile and vibrotactile displays for sensory substitution systems”, *IEEE Transactions on Biomedical Engineering*, Vol. 38, No. 1, pp. 1–16, 1991.
33. Jimenez, M. C. and J. A. Fishel, “Evaluation of Force, Vibration and Thermal Tactile Feedback in Prosthetic Limbs”, *2014 Ieee Haptics Symposium (Haptics)*, pp. 437–441, 2014.
34. Carey, S. L., M. Jason Highsmith, M. E. Maitland and R. V. Dubey, “Compensatory movements of transradial prosthesis users during common tasks”, *Clinical Biomechanics*, Vol. 23, No. 9, pp. 1128–1135, 2008.
35. Silcox, D. H., M. D. Rooks, R. R. Vogel and L. L. Fleming, “Myoelectric prostheses. A long-term follow-up and a study of the use of alternate prostheses.”, *The Journal of bone and joint surgery. American volume*, Vol. 75, No. 12, pp. 1781–9, dec 1993.
36. Hafshejani, M. K., M. Javanshir, M. Kamali, M. S. Ghasemi, M. Emami, S. A. Esmaeeli, A. Langari and M. Sattari Naeini, “The comparison of psychological and

- social adaptation below elbow amputation men using a mechanical and myoelectric prosthesis by using of TAPES questionnaire”, *Life Science Journal*, Vol. 9, No. 4, pp. 5583–5587, 2012.
37. Williams, T. W., “Progress on stabilizing and controlling powered upper-limb prostheses”, *Journal of Rehabilitation Research and Development*, Vol. 48, No. 6, pp. ix–xix, 2011.
 38. Biddiss, E., D. Beaton and T. Chau, “Consumer design priorities for upper limb prosthetics”, *Disability and Rehabilitation: Assistive Technology*, Vol. 2, No. 6, pp. 346–357, 2007.
 39. Resnik, L., M. R. Meucci, S. Lieberman-Klinger, C. Fantini, D. L. Kelty, R. Disla and N. Sasson, “Advanced upper limb prosthetic devices: Implications for upper limb prosthetic rehabilitation”, *Archives of Physical Medicine and Rehabilitation*, Vol. 93, No. 4, pp. 710–717, 2012.
 40. Schofield, J. S., K. R. Evans, J. P. Carey and J. S. Hebert, “Applications of sensory feedback in motorized upper extremity prosthesis: a review.”, *Expert review of medical devices*, Vol. 13, No. May 2016, pp. 1–13, 2014.
 41. Scott, R. N., “Feedback in myoelectric prostheses”, *Clinical Orthopaedics and Related Research*, Vol. 1, No. 256, pp. 58–63, 1990.
 42. Agur, A. M. R. and A. F. Dalley, *Grant’s atlas of anatomy*, Lippincott Williams & Wilkins, 2009.
 43. Johansson, R. S. and J. R. Flanagan, “Coding and use of tactile signals from the fingertips in object manipulation tasks.”, *Nature reviews. Neuroscience*, Vol. 10, No. 5, pp. 345–59, 2009.
 44. Edin, B. B., “Quantitative analysis of static strain sensitivity in human mechanoreceptors from hairy skin.”, *Journal of neurophysiology*, Vol. 67, No. 5, pp. 1105–1113, 1992.
 45. Bensmaia, S. and S. I. H. Tillery, “Tactile feedback from the hand”, *The Human Hand as an Inspiration for Robot Hand Development*, pp. 143–157, Springer, 2014.

46. Sherrington, C. S., *The integrative action of the nervous system*, CUP Archive, 1916.
47. Collins, D. and A. Prochazka, "Movement illusions evoked by ensemble cutaneous input from the dorsum of the human hand", *J. Physiol.*, Vol. 496, No. Pt 3, pp. 857–871, 1996.
48. Collins, D. F., K. M. Refshauge, G. Todd and S. C. Gandevia, "Cutaneous receptors contribute to kinesthesia at the index finger, elbow, and knee.", *Journal of neurophysiology*, Vol. 94, pp. 1699–1706, 2005.
49. Gandevia, S. C., J. L. Smith, M. Crawford, U. Proske and J. L. Taylor, "Motor commands contribute to human position sense.", *The Journal of physiology*, Vol. 571, No. Pt 3, pp. 703–710, 2006.
50. McCloskey, D. I., "Kinesthetic sensibility.", *Physiological Reviews*, Vol. 58, No. 4, pp. 763–820, 1978.
51. Kelso, J. A. S., "Motor control mechanisms underlying human movement reproduction", *Journal of Experimental Psychology. Human Perception and Performance*, Vol. 3, pp. 529–543, 1977.
52. Larish, D. D., C. M. Volp and S. a. Wallace, "An Empirical Note on Attaining a Spatial Target after Distorting the Initial Conditions of Movement via Muscle Vibration", *Journal of Motor Behavior*, Vol. 16, No. 1, pp. 76–83, 1984.
53. Srinivasan, M. A. and R. H. Lamotte, "Tactual discrimination of softness", *Journal of Neurophysiology*, Vol. 73, No. 1, pp. 88–101, 1995.
54. Hagert, E., M. Garcia-Elias, S. Forsgren and B. O. Ljung, "Immunohistochemical Analysis of Wrist Ligament Innervation in Relation to Their Structural Composition", *Journal of Hand Surgery*, Vol. 32, No. 1, pp. 30–36, 2007.
55. Kandel, E. R., J. H. Schwartz, T. M. Jessell, S. A. Siegelbaum and A. J. Hudspeth, *Principles of neural science*, Vol. 4, McGraw-hill New York, 2000.

56. Macefield, V. G., “Physiological characteristics of low-threshold mechanoreceptors in joints, muscle and skin in human subjects”, *Clinical and Experimental Pharmacology and Physiology*, Vol. 32, pp. 135–144, 2005.
57. Moraes, M. R. B., M. L. C. Cavalcante, J. A. D. Leite, F. V. Ferreira, A. J. O. Castro and M. G. Santana, “Histomorphometric evaluation of mechanoreceptors and free nerve endings in human lateral ankle ligaments”, *Foot & ankle international*, Vol. 29, No. 1, pp. 87–90, 2008.
58. Johansson, H., J. Pedersen, M. Bergenheim and M. Djupsjobacka, “Peripheral afferents of the knee: their effects on central mechanisms regulating muscle stiffness, joint stability, and proprioception and coordination”, *Proprioception and neuromuscular control in joint stability. Champaign, IL: Human Kinetics*, pp. 5–22, 2000.
59. Hughes, C. M. L., P. Tommasino, A. Budhota and D. Campolo, “Upper extremity proprioception in healthy aging and stroke populations, and the effects of therapist- and robot-based rehabilitation therapies on proprioceptive function.”, *Frontiers in human neuroscience*, Vol. 9, No. March, p. 120, 2015.
60. Hagert, E., “Proprioception of the Wrist Joint: A Review of Current Concepts and Possible Implications on the Rehabilitation of the Wrist”, *Journal of Hand Therapy*, Vol. 23, No. 1, pp. 2–17, 2010.
61. Proske, U. and S. C. Gandevia, “The kinaesthetic senses.”, *The Journal of physiology*, Vol. 587, No. Pt 17, pp. 4139–4146, 2009.
62. Sarlegna, F. R., G. M. Gauthier, C. Bourdin, J. L. Vercher and J. Blouin, “Internally driven control of reaching movements: A study on a proprioceptively deafferented subject”, *Brain Research Bulletin*, Vol. 69, No. 4, pp. 404–415, 2006.
63. Messier, J., S. Adamovich, M. Berkinblit, E. Tunik and H. Poizner, “Influence of movement speed on accuracy and coordination of reaching movements to memorized targets in three-dimensional space in a deafferented subject.”, *Experimental brain research*, Vol. 150, No. 4, pp. 399–416, 2003.

64. Adamo, D. E., B. J. Martin and S. H. Brown, "Age-related differences in upper limb proprioceptive acuity.", *Perceptual and motor skills*, Vol. 104, No. 3 Pt 2, pp. 1297–1309, 2007.
65. Ribeiro, F. and J. Oliveira, "Aging effects on joint proprioception: The role of physical activity in proprioception preservation", *European Review of Aging and Physical Activity*, Vol. 4, No. 2, pp. 71–76, 2007.
66. Gordon, J., M. F. Ghilardi and C. Ghez, "Impairments of reaching movements in patients without proprioception. I. Spatial errors.", *Journal of neurophysiology*, Vol. 73, No. 1, pp. 347–360, 1995.
67. Winward, C. E., P. W. Halligan and D. T. Wade, "Current practice and clinical relevance of somatosensory assessment after stroke.", *Clinical rehabilitation*, Vol. 13, No. 1, pp. 48–55, 1999.
68. Swash, M. and K. P. Fox, "The effect of age on human skeletal muscle studies of the morphology and innervation of muscle spindles", *Journal of the neurological sciences*, Vol. 16, No. 4, pp. 417–432, 1972.
69. Kim, J. S., "Patterns of sensory abnormality in cortical stroke: Evidence for a dichotomized sensory system", *Neurology*, Vol. 68, No. 3, pp. 174–180, 2007.
70. Kararizou, E., P. Manta, N. Kalfakis and D. Vassilopoulos, "Morphometric study of the human muscle spindle.", *Analytical and quantitative cytology and histology / the International Academy of Cytology [and] American Society of Cytology*, Vol. 27, No. 1, pp. 1–4, 2005.
71. Liu, J.-X., P.-O. Eriksson, L.-E. Thornell and F. Pedrosa-Domellöf, "Fiber content and myosin heavy chain composition of muscle spindles in aged human biceps brachii.", *The journal of histochemistry and cytochemistry : official journal of the Histochemistry Society*, Vol. 53, No. 4, pp. 445–454, 2005.
72. Seidler, R. D., J. A. Bernard, T. B. Burutolu, B. W. Fling, M. T. Gordon, J. T. Gwin, Y. Kwak and D. B. Lipps, "Motor control and aging: Links to age-related brain structural, functional, and biochemical effects", Vol. 34, No. 5, pp. 721–733, 2010.

73. Connell, L. a., N. B. Lincoln and K. a. Radford, “Somatosensory impairment after stroke: frequency of different deficits and their recovery”, *Clinical rehabilitation*, Vol. 22, No. 8, pp. 758–67, 2008.
74. Carey, L. M. and T. A. Matyas, “Frequency of discriminative sensory loss in the hand after stroke in a rehabilitation setting”, *Journal of Rehabilitation Medicine*, Vol. 43, No. 3, pp. 257–263, 2011.
75. Cho, S., J. Ku, Y. K. Cho, I. Y. Kim, Y. J. Kang, D. P. Jang and S. I. Kim, “Development of virtual reality proprioceptive rehabilitation system for stroke patients”, *Computer Methods and Programs in Biomedicine*, Vol. 113, No. 1, pp. 258–265, 2014.
76. Ramachandran, V. S. and W. Hirstein, “The perception of phantom limbs. The D. O. Hebb lecture”, *Brain*, Vol. 121, pp. 1603–1630, 1998.
77. Maidenbaum, S., S. Abboud and A. Amedi, “Sensory substitution: Closing the gap between basic research and widespread practical visual rehabilitation”, Vol. 41, pp. 3–15, 2014.
78. Gibson, A. and P. Artemiadis, “Neural closed-loop control of a hand prosthesis using cross-modal haptic feedback”, *IEEE International Conference on Rehabilitation Robotics*, Vol. 2015-Septe, pp. 37–42, 2015.
79. Amedi, a., R. Malach, T. Hendler, S. Peled and E. Zohary, “Visuo-haptic object-related activation in the ventral visual pathway.”, *Nature neuroscience*, Vol. 4, No. 3, pp. 324–330, 2001.
80. Frasnelli, J., O. Collignon, P. Voss and F. Lepore, “Crossmodal plasticity in sensory loss”, *Progress in Brain Research*, Vol. 191, pp. 233–249, 2011.
81. Striem-Amit, E., M. Guendelman and A. Amedi, “‘visual’ acuity of the congenitally blind using visual-to-auditory sensory substitution”, *PLoS ONE*, Vol. 7, No. 3, 2012.

82. Pylatiuk, C., S. Schulz and L. Döderlein, “Results of an Internet survey of myoelectric prosthetic hand users”, *Prosthetics and orthotics international*, Vol. 31, No. 4, pp. 362–370, 2007.
83. Cipriani, C., M. Dalonzo and M. C. Carrozza, “A miniature vibrotactile sensory substitution device for multifingered hand prosthetics”, *IEEE Transactions on Biomedical Engineering*, Vol. 59, No. 2, pp. 400–408, 2012.
84. Mahns, D. a., N. M. Perkins, V. Sahai, L. Robinson and M. J. Rowe, “Vibrotactile frequency discrimination in human hairy skin”, *Journal of neurophysiology*, Vol. 95, No. 3, pp. 1442–1450, 2006.
85. Walker, J. M., A. A. Blank, P. A. Shewokis and M. K. Omalley, “Tactile Feedback of Object Slip Facilitates Virtual Object Manipulation”, *IEEE Transactions on Haptics*, Vol. 8, No. 4, pp. 454–466, 2015.
86. Debus, T., T.-J. J. T.-J. Jang, P. Dupont and R. Howe, “Multi-channel vibrotactile display for teleoperated assembly”, *Proceedings 2002 IEEE International Conference on Robotics and Automation (Cat. No.02CH37292)*, Vol. 1, pp. 11–15, 2002.
87. Schoonmaker, R. E. and C. G. Cao, “Vibrotactile force feedback system for minimally invasive surgical procedures”, *2006 IEEE International Conference on Systems, Man and Cybernetics*, Vol. 3, pp. 2464–2469, 2006.
88. Okamoto, S., M. Konyo and S. Tadokoro, “Vibrotactile Stimuli Applied to Finger Pads as Biases for Perceived Inertial and Viscous Loads”, *IEEE Transactions on Haptics*, Vol. 4, No. 4, pp. 307–315, 2011.
89. Tappeiner, H. W., R. L. Klatzky, B. Unger and R. Hollis, “Good Vibrations: Asymmetric vibrations for directional haptic cues”, *Proceedings - 3rd Joint Euro-Haptics Conference and Symposium on Haptic Interfaces for Virtual Environment and Teleoperator Systems, World Haptics 2009*, pp. 285–289, 2009.
90. Fan Quek, Z., S. B. Schorr, I. Nisky, W. R. Provancher and A. M. Okamura, “Sensory substitution and augmentation using 3-degree-of-freedom skin deformation feedback”, *IEEE Transactions on Haptics*, Vol. 8, No. 2, pp. 209–221, 2015.

91. Gurari, N., K. Smith, M. Madhav and A. M. Okamura, "Environment discrimination with vibration feedback to the foot, arm, and fingertip", *2009 IEEE International Conference on Rehabilitation Robotics, ICORR 2009*, pp. 343–348, 2009.
92. Roll, J. P. and J. C. Gilhodes, "Proprioceptive sensory codes mediating movement trajectory perception: human hand vibration-induced drawing illusions.", *Canadian journal of physiology and pharmacology*, Vol. 73, No. 2, pp. 295–304, 1995.
93. Meek, S. G., S. C. Jacobsen and P. P. Goulding, "Extended physiologic taction: design and evaluation of a proportional force feedback system.", *Journal of rehabilitation research and development*, Vol. 26, No. 3, pp. 53–62, 1989.
94. Antfolk, C., A. Björkman, S. O. Frank, F. Sebelius, G. Lundborg and B. Rosen, "Sensory feedback from a prosthetic hand based on air-mediated pressure from the hand to the forearm skin", *Journal of Rehabilitation Medicine*, Vol. 44, No. 8, pp. 702–707, 2012.
95. Antfolk, C., M. D'Alonzo, M. Controzzi, G. Lundborg, B. Rosen, F. Sebelius and C. Cipriani, "Artificial redirection of sensation from prosthetic fingers to the phantom hand map on transradial amputees: Vibrotactile versus mechanotactile sensory feedback", *IEEE Transactions on Neural Systems and Rehabilitation Engineering*, Vol. 21, No. 1, pp. 112–120, 2013.
96. Stepp, C. E. and Y. Matsuoka, "Relative to direct haptic feedback, remote vibrotactile feedback improves but slows object manipulation", *2010 Annual International Conference of the IEEE Engineering in Medicine and Biology Society, EMBC'10*, pp. 2089–2092, 2010.
97. Bark, K., J. W. Wheeler, S. Premakumar and M. R. Cutkosky, "Comparison of Skin Stretch and Vibrotactile Stimulation for Feedback of Proprioceptive Information", *2008 Symposium on Haptic Interfaces for Virtual Environment and Teleoperator Systems*, pp. 71–78, 2008.

98. Wheeler, J., K. Bark, J. Savall and M. Cutkosky, “Investigation of Rotational Skin Stretch for Proprioceptive Feedback With Application to Myoelectric Systems”, *{IEEE} Transactions on Neural Systems and Rehabilitation Engineering*, Vol. 18, No. 1, pp. 58–66, 2010.
99. Meli, L., C. Pacchierotti and D. Prattichizzo, “Sensory subtraction in robot-assisted surgery: Fingertip skin deformation feedback to ensure safety and improve transparency in bimanual haptic interaction”, *IEEE Transactions on Biomedical Engineering*, Vol. 61, No. 4, pp. 1318–1327, 2014.
100. Schorr, S. B., Z. F. Quek, R. Y. Romano, I. Nisky, W. R. Provancher and A. M. Okamura, “Sensory substitution via cutaneous skin stretch feedback”, *Proceedings - IEEE International Conference on Robotics and Automation*, pp. 2341–2346, 2013.
101. Guinan, A. L., N. C. Hornbaker, M. N. Montandon, A. J. Doxon and W. R. Provancher, “Back-to-back skin stretch feedback for communicating five degree-of-freedom direction cues”, *2013 World Haptics Conference, WHC 2013*, pp. 13–18, 2013.
102. Provancher, W. R. and N. D. Sylvester, “Fingerpad Skin stretch increases the perception of virtual Friction”, *IEEE Transactions on Haptics*, Vol. 2, No. 4, pp. 212–223, 2009.
103. Pacchierotti, C., A. Tirmizi and D. Prattichizzo, “Improving transparency in teleoperation by means of cutaneous tactile force feedback.”, *ACM Transactions on Applied Perception*, Vol. 11, No. 1, pp. 1–16, 2014.
104. Beauchamp, M. S., “See me, hear me, touch me: Multisensory integration in lateral occipital-temporal cortex”, Vol. 15, No. 2, pp. 145–153, 2005.
105. Kitagawa, M., D. Dokko, A. M. Okamura and D. D. Yuh, “Effect of sensory substitution on suture-manipulation forces for robotic surgical systems”, *Journal of Thoracic and Cardiovascular Surgery*, Vol. 129, No. 1, pp. 151–158, 2005.

106. Gonzalez, J., H. Suzuki, N. Natsumi, M. Sekine and W. Yu, "Auditory display as a prosthetic hand sensory feedback for reaching and grasping tasks", *Proceedings of the Annual International Conference of the IEEE Engineering in Medicine and Biology Society, EMBS*, pp. 1789–1792, 2012.
107. Abboud, S., S. Hanassy, S. Levy-Tzedek, S. Maidenbaum and A. Amedi, "Eye-Music: Introducing a 'visual' colorful experience for the blind using auditory sensory substitution", *Restorative Neurology and Neuroscience*, Vol. 32, No. 2, pp. 247–257, 2014.
108. Lee, K. H., J. Ku, S. W. Jo, S. I. Kim, J. Y. Song, Y. J. Park, H. J. Kim and Y. J. Kang, "Upper extremity proprioceptive assessment test using virtual environment technique in patients with stroke", *Journal of Korean Academy of Rehabilitation Medicine*, Vol. 34, No. 2, pp. 141–149, 2010.
109. Brown, J. D., A. Paek, M. Syed, M. K. O'Malley, P. A. Shewokis, J. L. Contreras-Vidal, A. J. Davis and R. B. Gillespie, "An exploration of grip force regulation with a low-impedance myoelectric prosthesis featuring referred haptic feedback.", *Journal of neuroengineering and rehabilitation*, Vol. 12, p. 104, 2015.
110. Brown, J., M. Shelley, D. Gardner, E. A. Gansallo and R. Gillespie, "Non-colocated Kinesthetic Display Limits Compliance Discrimination in the Absence of Terminal Force Cues", *IEEE Transactions on Haptics*, Vol. PP, No. 99, pp. 1–1, 2016.
111. Casadio, M., P. Giannoni, P. Morasso and V. Sanguineti, "A proof of concept study for the integration of robot therapy with physiotherapy in the treatment of stroke patients.", *Clinical rehabilitation*, Vol. 23, No. 3, pp. 217–228, 2009.
112. Vergaro, E., M. Casadio, V. Squeri, P. Giannoni, P. Morasso and V. Sanguineti, "Self-adaptive robot training of stroke survivors for continuous tracking movements.", *Journal of neuroengineering and rehabilitation*, Vol. 7, p. 13, 2010.
113. Gonzalez-Badillo, G., H. I. Medellin-Castillo and T. Lim, "Development of a Haptic Virtual Reality System for Assembly Planning and Evaluation", *Procedia Technology*, Vol. 7, No. Theodore Lim, pp. 265–272, 2013.

114. Brough, J. E., M. Schwartz, S. K. Gupta, D. K. Anand, R. Kavetsky and R. Petersen, “Towards the development of a virtual environment-based training system for mechanical assembly operations”, Vol. 11, No. 4, pp. 189–206, 2007.
115. Boud, a. C., C. Baber and S. J. Steiner, “Virtual Reality: A Tool for Assembly?”, *Presence: Teleoperators and Virtual Environments*, Vol. 9, No. 5, pp. 486–496, 2000.
116. Oren, M., P. Carlson, S. Gilbert and J. M. Vance, “Puzzle assembly training: Real world vs. virtual environment”, *Proceedings - IEEE Virtual Reality*, pp. 27–30, 2012.
117. Williams II, R. L., M. Srivastava, J. N. Howell, R. R. Conatser Jr., D. C. Eland, J. M. Burns and A. G. Chila, “The virtual haptic back for palpatory training”, *ICMI'04 - Sixth International Conference on Multimodal Interfaces*, pp. 191–197, 2004.
118. Hergenhan, J., J. Rutschke, M. Uhl, S. E. Navarro, B. Hein and H. Worn, “A haptic display for tactile and kinesthetic feedback in a CHAI 3D palpation training scenario”, *2015 IEEE International Conference on Robotics and Biomimetics (ROBIO)*, pp. 291–296, IEEE, 2015.
119. Nakamura, T. and A. Yamamoto, “Multi-finger surface visuo-haptic rendering using electrostatic stimulation with force-direction sensing gloves”, *IEEE Haptics Symposium, HAPTICS*, pp. 489–491, 2014.
120. Xu, C., H. Li, K. Wang, J. Liu and N. Yu, “A bilateral rehabilitation method for arm coordination and manipulation function with gesture and haptic interfaces”, *2015 IEEE International Conference on Robotics and Biomimetics (ROBIO)*, pp. 309–313, IEEE, 2015.
121. Comas, O., Z. A. Taylor, J. Allard, S. Ourselin, S. Cotin and J. Passenger, “Efficient nonlinear FEM for soft tissue modelling and its GPU implementation within the open source framework SOFA”, *Lecture Notes in Computer Science (including subseries Lecture Notes in Artificial Intelligence and Lecture Notes in Bioinformatics)*, Vol. 5104 LNCS, pp. 28–39, 2008.

122. Talbot, H., N. Haouchine, I. Peterlik, J. Dequidt, C. Duriez, H. Delingette and S. Cotin, “Surgery Training, Planning and Guidance Using the SOFA Framework”, *Eurographics*, 2015.
123. Gurari, N., K. J. Kuchenbecker and A. M. Okamura, “Perception of springs with visual and proprioceptive motion cues: Implications for prosthetics”, *IEEE Transactions on Human-Machine Systems*, Vol. 43, No. 1, pp. 102–114, 2013.
124. Chatterjee, A., P. Chaubey, J. Martin and N. Thakor, “Testing a Prosthetic Haptic Feedback Simulator With an Interactive Force Matching Task”, *JPO Journal of Prosthetics and Orthotics*, Vol. 20, No. 2, pp. 27–34, 2008.
125. Samur, E., “Systematic evaluation methodology and performance metrics for haptic interfaces”, *World Haptics Conference (WHC), 2011 IEEE*, p. 1, IEEE, 2011.